Answers to anonymous Referee #1

Please note that our answers are written to each comment in italic type.

General comments In the manuscript bg-2017-119 presents some important new data on early diagenetic properties and carbon mineralization in the Laptev and East Siberian Sea shelf and slope sediment. In my opinion, it should eventually be published but requires at least moderate revision. Generally, data set is interesting and solid, and conclusions are believable, but the discussion part is a bit unfocussed and manuscript needs to be more concise. In addition, I would suggest that the effect of physical activities such as resuspention and redeposition on pore-water solute concentrations in some shallow sites should be discussed in this manuscript.

Specific comments

(1) line 207 The boundary conditions of the reaction-transport model should be shown in 2.5.

Answer: We will provide the boundary conditions for the model runs in a table in the appendix.

(2) Line 210 Generally, the diffusion process includes molecular diffusion and bioturbation, and is not related to bioirrigation. If the study area has evident bioirrigation process, the bioirrigation term a(C0-C) should be added to the model (a is the irrigation coefficient).

Answer: We have tested the model fits with and without bioirrigation and found no improved fit to the measured concentration data when bioirrigation was included as a process. The exception to this is only Station 48.

(3) Table 2 showed that DIC fluxes are apparently lower than oxygen uptake rates , but as far as I know, oxygen uptake rates were similar or lower than DIC fluxes in many estuarine and shelf regions. Are there any important processes for removing the porewater DIC in your study regions? Please explain more about the differences between DIC fluxes and oxygen uptake rates.

Answer: The most likely explanation for the lower DIC fluxes is probably the difference in methods used for the two measurements. With the 1-cm depth resolution of the porewater analyses we are not capturing the gradient in the topmost cm of sediment, the depth at which under aerobic conditions $CaCO_3$ dissolution may take place that would otherwise explain higher or equal DIC to O_2 fluxes. The measured gradent is therefore produced by the low anaerobic carbon mineralization rates below 1 cm sediment depth. Based on major ion analysis of Ca^{2+} and Mg^{2+} we see no evidence of cation removal that may be associated with carbonate precipitation. We therefore argue that the lower DIC than O_2 fluxes are a consequence of the different measuring methods that use different vertical resolutions. In support of our assessment, we have now added the DIC fluxes measured for the whole-core incubations that were also used to measured the total O_2 uptake with 2D optodes and added these to Table 2. There is very good agreement between the whole core DIC fluxes and the O_2 uptake rates, consistent with high mineralization rates in the topmost cm of sediment and minimal $CaCO_3$ dissolution.

(4) Line 371 Pore-water DIC/NH4+ ratios should be corrected by diffusion and adsorption process or at least the authors should demonstrate that these processes can be neglected.

Thank you for pointing this out. We will correct our rates by accounting for the difference in diffusion coefficients between NH_4^+ and DIC (HCO_3^-) and the adsorption coefficient of NH_4^+. We would like to point out that this correction has a negligible effect on our data analysis because of the similarity in diffusion coefficients and the small correction for ammonium adsorption.

(5) Line 639 In general, the net Corg settling rates equal to sum of 210Pb-based Corg mass accumulation rates and oxygen uptake rates if the sedimentary Corg changed little with depth, and thus 210Pb-based Corg mass accumulation rates can be lower or higher than oxygen uptake rates.

Answer: Thank you. We agree. If samples for Pb-210 dating are taken at 1-cm resolution and the topmost cm is either not sampled cleanly or includes a C-rich flocculen tlayer that is not a large total volume of that depth interval, the true carbon inventory is underestimated and deviations such as the ones we observe arise.

(6) Line 672 Some shelf stations which were influenced by bioturbation should be written, and these discussions about mixing process look like contrasting with the results of optimal fits of the concentration profiles (line 388). Please explain more about the mixing process.

Answer: We will make this clearer by adding a table on the model optimization to an appendix, in which we will present the bioturbation and bioirrigation coefficients.

(7) Line747 It is difficult to build relationship with priming effect based on existing data in this paper unless you can find more relevant evidence.

Answer: We agree. In response to both reviewers' comments we will remove the treatment of potential priming in the Laptev Sea.

(8) Conclusions are too long and not concise, which need to be modified. I would suggest some contents in conclusions could be incorporated into discussion part.

Answer: We will sharpen the conclusions and shorten them, but want to use this section to provide a broader perspective of our study.

Technical corrections

(1) Line 119 'A fifth core' should be 'A fourth core'
Answer: Corrected. The fifth core occurred when duplicate cores were taken for porewater measurements.

(2) I would suggest that r2 and p should be shown in the Fig. 9.

Answer: We will include this information.

Reply to anonymous Referee #2

Please note that our answers are written to each comment in italic type.

The manuscript "Carbon mineralization in Laptev Sea and East Siberian Sea shelf and slope sediment" of Brüchert and co-workers describes interesting sediment data from 19 different stations in the East Siberian Sea. The authors measured depth profiles of geochemical data such as DIC concentrations and their stable isotope signatures, oxygen, sulfate and ammonium concentrations as well as process data of sulfate reduction and oxygen consumption. Furthermore, they used the profile data of manganese and iron to model manganese and iron reduction rates. Based on DIC stable isotope signatures and the fraction of DIC from organic matter mineralization they derived the contribution of marine and terrestrial organic matter to overall organic matter decomposition using a common endmember model. Finally they upscaled their data to the outer Laptev Sea and the outer East Siberian Sea. This is an impressive data set from a region, which is only hardly accessible and of which only few data are available. The presented data are of great interest for readers of Biogeosciences and worth being published.

However, the presentation and interpretation of the data need substantial improvement. The manuscript is very long and contains substantial reiterations. But more importantly, a part of the manuscript has the classical structure of Introduction, M&M, Results and Discussion, but a large fraction of Methods and Results is presented in the Discussion only.

Answer: We appreciate the reviewer's view of our manuscript structure. However, the part of the discussion the reviewer refers to includes the development of a mass balance model to assess the marine versus terrestrial organic matter contribution to degradation. As such, the mass balance model approach should not be seen as part of the analytical materials and methods, but as a quantitative discussion of our analytical results including the development of model equations. For example, the derivation of the slope and intercept in the DIC versus $\delta^{13}C_{DIC}$ plots is not possible without prior analytical results, and neither is the derivation of the relative contributions of marine and terrestrial matter possible without prior analysis of total fluxes. We feel that splitting this part into the materials and methods section and in the discussion section would actually not reduce, but increase the length of the manuscript without adding clarity and lead to dissected information. We would therefore like to retain the present structure in some parts. However, there are other parts, where we agree with the reviewer and these sections will be moved to results and methods, where appropriate.*

Some results are even discussed before Methods and Results are presented, which makes the manuscript hard to read. I suggest thoroughly rearranging the manuscript according to the classical structure of research manuscripts and shortening the manuscript by removing reiterations.

Answer: We will try to find all unnecessary repeats and remove them to shorten the manuscript as much as possible.

In particular, the description of the authors approach of partitioning total organic carbon degradation into terrestrial and marine sources needs substantial attention and should be clearly divided into a description of Methods, Results and Discussion (see below).

Answer: Please see our comment above. The derivation of the equations shoul be part of the discussion to aid in the flow of the argument in the discussion text, but we will, for examle, move parts of the reaction transport model and the carbon equivalent assignment of anaerobic carbon degradation to the methods and results.

In this context, I missed the carbon concentrations in the sediments and their stable

isotope signatures. I assume the authors measured them and they will help to interpret the results of the "modelled" _13C signatures of respired organic matter.

Answer: Yes, we have concentrations and $\delta^{13}C_{org}$ values for some, but not all sediments. We have revised the manuscript to cite these references where data are available (some weren't citeable at the time of the original writing, but are now. Since the manuscript already has many data we chose to focus on the novel rates and porewater chemistry instead. There are already a number of publications of the C_{org} and $\delta^{13}C$ contents of these sediments (e.g., Vonk et al, 2012; Bröder et al., 2016 a,b, Karlsson et al. (2015), Salvado et al., 2016) and we wished not to reiterate similar data that were already published.

Most of the data seem being related to anoxic carbon degradation processes, excluding aerobic organic matter turnover, although oxic processes are responsible for most of the organic carbon decomposition in the studied sediments. The authors should clarify throughout the whole manuscript if they relate to total, oxic or anoxic carbon decomposition.

Answer: Although we have been very clear to our opinion in distinguishing the aerobic from the anaerobic degradation processes, we will carefully reevaluate the text where this distinction may be obscure.

The conclusions are very long and mainly a reiteration of the results and the discussion. It should be shortened substantially.

Answer: We will carefully evaluate where re-iterations occur and remove them, when necessary. However, we do not agree with the reviewer that our conclusions just reiterate the results. Instead, the conclusions put the discussion into the greater context of the overall Arctic marine carbon cycle and some of the debated questions on the likelihood whether sediment-based terrestrial carbon degradation contributes ocean acidification in this region.

Specific comments:
L 29: Please give the depth used for integrating

Answer: 30 cm of sediment; revised

L 48: These C amounts are stored in soils of permafrost landscapes. In the permafrost itself only 800 Pg are stored, see Hugelius et al. 2014. Please rephrase.

Answer: Hugelius et al (2014) state that 800 Pg are in perennially frozen permafrost, whereas they state that the estimated SOC storage ranges ranges between 1100 to 1500 Pg. We are referring to the latter number.

L 56: "qualitatively different rates" is unclear, please rephrase.

Answer: We agree that qualitative is vague, but this is because the literature is often vague on rate constants. Here the term 'qualitative' refers to the widely used characterization of very reactive as opposed to unreactive organic material without specific reference to a degradation rate constant.

L 146 omit one "dissolved"

Done.

L 154-155: This is a reiteration from 2.1; please remove one of the descriptions.

Answer: removed "undisturbed sediment surfaces and ..".

L 176 – 200: Please indicate where the measurements were done (on the ship, in the home lab) and how the samples were transported.

We have inserted the following sentence: Ammonium was determined on a QUAATRO 4-channel flow injection analyzer (Seal Analytical) on board. All other porewater analyses were performed at the Department of Geological Sciences, Stockholm University. Samples that were analyzed in the home laboratory remained cold or frozen on board until arrival of the icebreaker Oden in Sweden

L221-223: Reiteration from 2.1, please remove one of the descriptions.

Removed one "concentration"

L256: Please describe how texture was determined.

Answer: This is a qualitative descriptor of the sediment based on visual inspection. No detailed grain analysis was performed.

L 257: The designation of colors throughout the sediment description is not unambiguous. Please use an accepted color system such as Munsels.

Munsell's colour chart was not used in the description. Unfortunately, we do not have sediment cores left to compare these to a colour chart. We have instead used colour descriptions that are commonly used for describing sediment cores from the Ocean Drilling Program.

L 296: These data are not presented in Table 2 and it seems they are not presented in the manuscript at all.

We inserted these numbers into Table 2 (modelled/measured) O2 uptake

L 341-342: Please identify the station.

Inserted: Stations 6 to 24

L 352-356: Here the presentation of the carbon concentration data are needed. Furthermore, to better illustrate changes in organic matter reactivity, SRR should also be presented normalized to organic carbon.

For information, the $\delta^{13}C$ of these sediments vary between -26 ‰ in the Laptev Sea to -20 in the easternmost Siberian Sea (Salvado et al., 2016, Biogeosciences). The carbon concentrations on the outer shelf vary between 0.4% and 1.5% (Bröder et al., 2016b Org. Geochem, Salvado et al., Biogeosciences, pers. data, unpubl.).

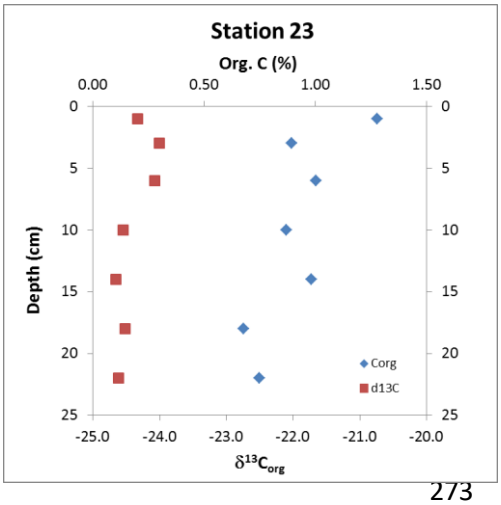

We attach here a depth profile of organic carbon (%) and $\delta^{13}C_{org}$ from Station 23 to support our point. There is little variation in the $\delta^{13}C$ data with depth. C_{org} concentrations decrease from about 1.3% to 0.8 %, a 40% decrease. Similar profiles can be found in Bröder et al (2016b, Org. Geochem.). It may be argued that the higher C_{org} concentrations in the topmost cm reflect more degradable organic matter, but the decrease in the actual anaerobic degradation rates with depth (Fig. 3) is much larger, more than a factor 8! Scaling the rates to C_{org} concentrations therefore will show the same trend and imply that the reactivity refers to the bulk org. C, which in fact is not true. We have chosen instead to use the conventional unit of ^{35}S-sulfate reduction rates per volume sediment (nmol cm^{-3} d^{-1}), which allows comparison of these rates to the large global database of marine ^{35}S-sulfate reduction rates.

L 360: Decrease or increase of DIC? Furthermore, data of Station 50 should be presented in Fig. 4 if they are given in the text.

Answer: Decrease was corrected. We meant "increase"

L 368: Please indicate where the rates of sedimentation are shown.

Answer: We have removed 'sedimentation' from the sentence. We infer that sedimentation rates would have decreased abruptly at this depth, because the change in sulfate reduction rates over 1 cm depth cannot be explained by a steady exponential decrease in organic matter reactivity.

L 381-387: This are results that should be presented in the Results section.

Answer: The mixing coefficients derived here are the result of the optimization procedure and a specific result for the different stations and will be moved there. We therefore propose to move the reactive transport modeling results into the results section.

L 395: This is a discussion of results that were not shown. Please show these results in the Results section before discussing them.

Answer: See above.

L 418: Table 4L 488-502: This is a description of methods, which should go to the Methods.

Answer: We will add a section to the materials and methods on the calculation of the carbon equivalents

L 498: Please clarify “no or very minor”. Was isotope fractionation considered or not?

Answer: It was not.

L 500: What means minor. Please show the formula for the calculations.

Answer: Minor to the extent that it cannot be analytically detected based on Ca^{2+} and Mg^{2+} porewater concentration decreases. The calculation refers to equation (3) in line 492.

L 502-506: This should go to the Results.

Answer: We will move this sentence to the results.

L 505: -35.8‰ is a very low stable isotope value for organic matter, even lower than found for terrestrial organic matter in the hinterland of the Laptev Sea. To assess the significance of this value the stable isotope signatures of the bulk organic matter are needed. Is it possible that methane oxidation contributed to DIC? Are methane concentration values available and can they be referred to?

Answer: Miller et al. 2016 (Biogeosciences) discuss this issue extensively and have come to the conclusion that methane in general and methane oxidation play no role for the porewater chemistry on the East Siberian slope. We were also surprised by the strong decrease with depth in $\delta^{13}C$ DIC. To check the validity of our results we have simulated depth profiles of DIC assuming degradation of a terrestrial organic matter component with an isotope composition of -28‰. However, such a heavy component requires substantially higher carbon degradation rates to match the decrease in $\delta^{13}C$ of DIC, which does not agree with the rates of oxygen uptake, iron and manganese and sulfate reduction measured here. Further, we considered whether there was loss of ^{13}C by precipitation of $CaCO_3$ from porewater. This is, however, also not substantiated based on Ca^{2+} and Mg^{2+} porewater concentrations and the greater likelihood for $CaCO_3$ dissolution than precipitation under the conditions on the lower slope at 3146 m water depth. Given that there are no good alternative explanations or handling artefacts, we present these values as indicating a strongly ^{13}C-depleted terrestrial signature, although the bulk $\delta^{13}C_{org}$ for this station (Tesi, unpubl. Data) is around -24 to -25‰.

L 525- 538: This is a method description and should go to the Methods

Answer: For the sake of the flow of the discussion, we would like to retain this section in place. It is part of our analytical approach to discussing our data and should not be seen as being strictly part of the analytical section of the raw data.

L 539 – L542: These data should be presented in the results.

Answer: We argue for the same reason as above to retain this part.

L 545 – 570: This paragraph again contains mostly a description of methods. The description was also not completely clear to me. Better present the respective formula used for partitioning degradation rates into terrestrial and marine sources. Furthermore, I understood that the authors only considered organic matter degradation via sulfate reduction. If this is the case, it should be made clear, that this approach gives no information on most of organic

matter degradation in the sediments (aerobic processes), which likely consume the most labile fraction of deposited organic matter.

Answer: To our knowledge, this is the first time such an approach has been used to extract specific marine and terrestrial carbon fraction degradation rates. The reviewer is correct and this is what we have stated in the text.

L 571 – 573: I cannot see that the data in Fig. 7 shows the "influence of offshore transport of terrestrial organic matter". The figure rather shows decreasing O2 consumption rates and SRR from the shelf down the slope. Please clarify. Furthermore, the remineralized DIC 13C data from Table 3 rather show increasing terrestrial influence down the slope. How does this relate to the data in Fig. 7?

Answer: The sentence is intended to provide an explanation for the observed decrease. As discussed earlier in the text, terrestrial organic matter is transported offshore and molecular organic studies have shown that the reactivity of this organic matter decreases offshore, consistent with the observed decrease. The $\delta^{13}C_{DIC}$ data from the slope reflect the carbon degradation processes in deeper, buried sediment. These are apparently to a large extent driven by terrestrial organic matter degradation, albeit at low rates.

L 606: outer Siberian shelf sediment

Answer: corrected

L 609: Please show the carbon data in the Results.

Answer: Carbon concentration data can be found in Bröder et al (2016) Biogeosciences and Salvado et al (2016) Biogeosciences. We added a citation to the text.

L 622 – 627: This should go to the Methods. Please clarify how the "degradation rate constant of organic matter" (L 620) can be determined by the anaerobic carbon mineralization (L 622) if latter only contributes 4 to 26% to total organic matter turnover in the sediments (Table 4).

Answer: We move the analytical approach of this section to the methods section. We are specific that this is the anaerobic degradation rate constant. We also show that the oxygen consumption rates are significantly faster than the anaerobic rates, but our isotope approach cannot resolve the origin of the carbon used for aerobic respiration. We agree with Boetius and Damm (1998) that in principle the marine export is large enough to account for all the oxygen uptake, but this does not disprove that a fraction of terrestrial organic matter is also degraded aerobically. Unfortunately, we cannot resolve this question satisfactorily.

L 635: anoxic degradation rate measurements?

Answer: Yes, anaerobic degradation rates is what is meant here.

L 648-650: This sentence should be rephrased since it is unclear. Which implications? If only anaerobic degradation rates are used in the assessment, isn't it obvious that no information on aerobic decomposition can be derived?

Answer: We will rephrase this sentence. It is important to point out explicitly that all common field measurements of O_2 consumption at the sediment surface cannot distinguish a marine from a terrestrial carbon contribution for a mixed source. We feel this is an important point to make, because degradation of terrestrial-derived carbon can only be achieved with additional

experiments using isolated sediment from only the oxygenated layer of the sediment. Given that this layer is only a few millimeters thick, this is not a trivial task and could not be achieved within the framework of this study. Nevertheless, we provide a range of previously unknown baseline data for this region, but want to point that other existing published assessments of terrestrial carbon degradation rates on the Siberian shelf are insufficiently constrained.

L 654 – 656: These results should go to the Results section.

Answer: This section will be moved to the results.

L 654 – 661: Where are these data shown? Only in text of the discussion?

Answer: This section will be moved to the results.

L 659: This sentence is unclear. Regression line of which data? How do you come from a slope of 5.6 to 18%?

Answer: This is the inverse of the slope of 5.6

L 663 – 664: The numbers for the contribution of anaerobic organic matter decomposition to total organic matter decomposition are given in Table 4 and are generally lower than 18%. This should be discussed.

Answer: This is the consequence of two methods, (1) the regression analysis and (2) the carbon equivalent apportionnement of the anaerobic degradation processes.

L 664 – 666: I cannot follow this conclusion. If the contribution of anaerobic organic matter decomposition is only slightly lower (L 661) this means only that (relatively) more organic matter is degraded aerobically but I do not see any information on "highly reactive marine-derived organic material". Please rephrase.

Answer: We try to clarify this by modifying the sentence. In case there is a misunderstanding, an explanation needs to be found for why there should be a greater proportion of aerobic respiration in the Siberian shelf sediment compared to other shelf sediments. We think a viable explanation is that there is a highly reactive marine fraction in the topmost millimeters of sediment that is not present any longer in the buried sediment, where very unreactive terrestrial organic matter prevails. Most shelf sediments with stronger marine C_{org} contributions in temperate regions would not have such a binomial Corg origin of widely different reactivities and a greater proportion of marine Corg would be buried. Hence, the reducing equivalents produced by anaerobic respiration in the Siberian shelf sediment make up a proportionately smaller fraction of the oxygen consumption compared to other shelf environments.

L 711 – 712: Can these data please be presented in the Results?

Answer: Our rates were compared with the figures in Bourgeois et al (2017). These are largely interpolated results or derived from the rates by Boetius and Damm (1998), which are already part of Figure 7 A, B.

L 725 – 728: As I understand this relates only to anaerobic organic carbon mineralization. Please clarify.

Yes, this is true. For the reasons that the fine-scale processes in the aerobic zone are not resolvable with the porewater analysis used here, the modelling of the porewaters refers to the anaerobic processes.

L 748 – 151: This sentence is unclear. The manuscript did not present any data on priming. How would priming be assessed by this dataset? How can priming be "deduced from the dual contribution of terrestrial and marine-derived organic matter to DIC"? I suggest omitting any reference to priming or show a dataset that relates to priming.

Answer: We will remove the discussion on priming.

L 1127-1129: Please quote the respective reference.

Answer: The data are from Canfield et al., 2005; Aquatic Geomicrobiology; we will add this.

Table 2: Please give mean values also for SRR and O2 uptake at the East Siberian Shelf and standard deviations for all mean values. Furthermore, indicate why a part of the data are missing.

Answer: In the revised version, this has now been done. In addition, we show values from the total oxygen uptake and for the DIC flux based on the whole-core flux experiments.

Table 5: please explain TEAP

Answer: TEAP are Terminal Electron-Accepting Processes after Stumm and Morgan (2006) Aquatic Chemistry; We have added the full term to the text.

Figures 2-5: please give the legend at least in one of the panels.

Fig. 4 + 5: The _-symbol in the axis name is missing

Answer: This is a conversion error from Excel to pdf. We will correct this.

Carbon mineralization in Laptev and East Siberian Sea shelf and slope sediment

Volker Brüchert[1,3], Lisa Bröder[2,3], Joanna E. Sawicka[1,3], Tommaso Tesi[2,3,5], Samantha P. Joye[6], Xiaole Sun[4,5], Igor P. Semiletov[7,8,9], Vladimir A. Samarkin[6]

[1] Department of Geological Sciences, Stockholm University, Stockholm, Sweden
[2] Department of Environmental Sciences and Analytical Chemistry, Stockholm University, Stockholm, Sweden
[3] Bolin Centre for Climate Research, Stockholm University, Stockholm, Sweden
[4] Baltic Sea Research Center, Stockholm University, Stockholm, Sweden
[5] Institute of Marine Sciences – National Research Council, Bologna, Italy
[6] Department of Marine Sciences, University of Georgia, Athens, U.S.A.
[7] International Arctic Research Center, University Alaska Fairbanks, Fairbanks, USA
[8] Pacific Oceanological Institute, Russian Academy of Sciences, Vladivostok, Russia
[9] Tomsk National Research Politechnical University, Tomsk, Russia

Abstract The Siberian Arctic Sea shelf and slope is a key region for the degradation of terrestrial organic material transported from the organic carbon-rich permafrost regions of Siberia. We report on sediment carbon mineralization rates based on O_2 microelectrode profiling, intact sediment core incubations, ^{35}S-sulfate tracer experiments, porewater dissolved inorganic carbon (DIC), $\delta^{13}C_{DIC}$, and iron, manganese, and ammonium concentrations from 20 shelf and slope stations. This data set provides a spatial overview of sediment carbon mineralization rates and pathways over large parts of the outer Laptev and East Siberian Arctic shelf and slope and allowed us to assess degradation rates and efficiency of carbon burial in these sediments. Rates of oxygen uptake and iron and manganese reduction were comparable to temperate shelf and slope environments, but bacterial sulfate reduction rates were comparatively low. In the topmost 20 to 50 cm of sediment, aerobic carbon mineralization dominated degradation and comprised on average 84% of the depth-integrated carbon mineralization. Oxygen uptake rates and ^{35}S-sulfate reduction rates integrated over the topmost 30 cm of sediment were higher in the eastern East Siberian Sea shelf compared to the Laptev Sea shelf. DIC/NH_4^+ ratios in porewaters and the stable carbon isotope composition of remineralized DIC indicated that the degraded organic matter on the

Siberian shelf and slope was a mixture of marine and terrestrial organic matter. Based on dual end member calculations, the terrestrial organic carbon contribution varied between 32% and 36%, with a higher contribution in the Laptev Sea than in the East Siberian Sea. Extrapolation of the measured degradation rates using isotope end member apportionment over the outer shelf of the Laptev and East Siberian Sea suggests that about 16 Tg C per year are respired in the outer shelf sea floor sediment. Of the organic matter buried below the oxygen penetration depth, between 0.6 and 1.3 Tg C per year are degraded by anaerobic processes, with a terrestrial organic carbon contribution ranging between 0.3 and 0.5 Tg per year.

Key words: Carbon mineralization, Arctic shelf and slope sediment, Laptev Sea, East Siberian Sea

1. Introduction

The biogeochemical fate of terrestrial organic carbon deposited on the Arctic shelf and slope is one of the most important open questions for the marine Arctic carbon cycle (e.g., Tesi et al., 2014; Macdonald et al., 2015; McGuire et al., 2009; Vonk et al, 2012). The total pan-Arctic terrestrial permafrost carbon reservoir has been estimated at about 1100 – 1500 Pg (Hugelius et al, 2014) – a carbon pool large enough to substantially affect the global atmospheric carbon dioxide pool over the next 100 years, even when only partially decomposed after thawing and oxidation (Schuur et al. 2015; Koven et al., 2015). Yet, there remains considerable uncertainty regarding the mineralization of terrestrial organic matter exported by rivers and coastal erosion to the Siberian shelf and slope (Tesi et al., 2014; Karlsson et al. 2015; Semiletov et al., 2011; Salvado et al., 2016).

Terrestrial organic matter transported to the Siberian shelf is of variable size, age, and molecular composition, which results in a range of qualitatively different carbon degradation rates of bulk carbon and individual molecular components. Size class analysis of the organic matter suggests that coarse organic material settles preferentially in near-shore environments, whereas finer organic fractions disperse offshore in repeated deposition-resuspension cycles gradually losing particular molecular components and overall reactivity (Wegner et al., 2013; Tesi et al., 2014, 2016). Substantial oxic degradation of organic matter may occur during near-bottom transport in resuspension-deposition cycles across the shelf (Bröder et al., 2016a). Up to 90% of certain biomarker classes may decompose during transport, whereby

most of the degradation may take place while the transported organic material resides in the sediment before being resuspended (Bröder et al., 2016a). However, without making approximations on transport direction, particle travel time and travel distance these studies cannot provide direct insights into the rates of carbon degradation and resultant CO_2 fluxes from sediment. By contrast, direct kinetic constraints provided by sediment carbon degradation rates can provide testable data for coupled hydrodynamic biogeochemical models that help assess the fate of land-exported terrestrial carbon pool on the Siberian shelf.

Relatively few studies have directly measured rates of carbon mineralization rates in Siberian shelf sediment (e.g., Boetius and Damm, 1998; Grebmeier et al., 2006; Karlsson et al., 2015, Savvichev et al., 2007). Boetius and Damm (1998) used high-resolution oxygen microelectrode data to determine the surface oxygen concentration gradients and oxygen penetration depths in a large number of sediment cores from the shelf and slope of the Laptev Sea. Based on corresponding sediment trap and export productivity data, they concluded that the annual marine organic carbon export in the Laptev Sea shelf and slope was sufficiently high to explain the observed oxygen uptake rates. Current understanding therefore holds that due to the long annual ice cover and low productivity on the eastern Siberian Arctic shelf and slope, only a small amount of marine organic carbon is exported and buried in Laptev and East Siberian Sea shelf sediment. The highly reactive fraction of fresh organic matter is thought to degrade in the surface sediment (Boetius and Damm, 1998). Consequently, anaerobic respiration in buried sediment has been thought to be negligible and to reflect the degradation of unreactive terrestrially derived carbon compounds. To our knowledge, with the exception of a recent study by Karlsson et al (2015) a more direct assessment of terrestrial carbon-derived mineralization rates in buried shelf and slope sediment has not been reported for the East Siberian Arctic Sea.

In this study, we present data from oxygen microelectrode profiling experiments, porewater data of dissolved inorganic carbon and its stable carbon isotope composition, and ^{35}S-sulfate reduction rate experiments along a shelf-slope transect near 125°E in the Laptev Sea. Samples were taken during the summer 2014 on the SWERUS-C3 expedition with the Swedish icebreaker Oden. We combined these data with porewater analyses of dissolved ammonium, sulfate, iron, and manganese to assess the major carbon degradation pathways and rates across the extensive outer Laptev and Siberian shelf and slope.

2. Materials and methods

2.1. Sample collection

Samples were collected at 20 stations from 40 to 3146 m water depth in the western Laptev and East Siberian Sea (Fig. 1 and Table 1). In this study we only report on sampling sites that showed no methane gas plumes, acoustic anomalies in the water column, or sediment blankings indicative of rising gas. In areas of active ebullition from the seafloor as seen by video imagery and acoustic gas blankings in the water column, the biogeochemistry of sea floor processes such as bacterial sulfate reduction, DIC concentration and its carbon isotope composition, and oxygen uptake are affected by methane oxidation. These methane cycling-related signals overprint the biogeochemistry imparted by carbon mineralization and are reported in a separate study.

Sediment stations had variable ice cover (Table 1). In the Laptev Sea, except for the deep-water slope stations between 3146 m and 2106m, all stations had open water. By contrast, ice cover exceeded 75% in the East Siberian Sea to the west and east of Bennett island (Station 40 to 63). Sediments with well-preserved sediment surfaces were collected with a Multicorer (Oktopus GmbH, Kiel, Germany) that simultaneously takes 8 sediment cores over an area of about 0.36 m^2 with acrylic tubes (9.5 cm diameter, 60 cm length) to 40 cm depth preserving clear water on top of the sediment. At stations 6, 23, and 24, an underwater video system (Group B Distribution Inc., Jensen Beach, U.S.A.) was mounted on the multicore frame to record the deployment and recovery, and to document the sea floor habitat. For the investigations all cores were taken from the same cast. Two of the cores were used to determine ^{35}S-sulfate reduction rates and porosity. In addition, one core with predrilled 3.8 mm holes sealed with electric tape was used to extract porewaters with rhizons (Rhizosphere Research Products BV, Wageningen, Netherlands). A fourth core was used for microelectrode measurements of dissolved oxygen concentration profiling, and finally, four other cores were used for whole-core incubations to determine benthic fluxes of dissolved oxygen, dissolved inorganic carbon, and nutrients. The cores were capped with rubber stoppers until further subsampling usually within 30 minutes. For sulfate reduction rates, the cores were subsampled with 40 or 50 cm long acrylic tubes (26 mm inner diameter) prepared with silicon-sealed holes, drilled at distances of 1 cm. For whole-core incubations, the cores were sub-sampled with 25 cm-long, 60 mm-wide tubes (56 mm id) to 12 cm depth. Likewise, a 60 mm diameter tube (56 mm id) was collected for microelectrode measurements preserving

about 3 cm of the overlying bottom water. For intact whole-core incubations, temperature-controlled aquaria were filled with bottom water that was collected from a CTD rosette from the same station by collecting water from four ten-liter rosette bottles usually ~5 meters above the sea floor. All sediment cores were closed with a stopper retaining the water on top of the sediment and stored at 1.5°C in an incubator until further processing.

2.2. Microelectrode oxygen profiles

High-resolution O_2-profiles across the water-sediment interface were obtained to determine oxygen penetration depths and diffusive oxygen uptake (Rasmussen and Jørgensen, 1992; Glud, 2008) (Table 2). The 60 mm tubes were placed in an aquarium filled with bottom water from the same station, overflowing the sediment core. The water temperature was kept to ~1°C by a cooling unit (Julabo GmbH, Seelbach, Germany). In exceptional cases when there was not sufficient bottom water available to fill the aquarium, bottom water was used from a pump system. A stable diffusive boundary layer above the sediment was created by passing air from an aquarium pump over the water surface with a Pasteur pipette creating a slow rotational motion of water inside the core. At each station six to eight O_2 microprofiles were measured using Clark-type oxygen microelectrodes (OX-50, Unisense, Århus Denmark) mounted on a motor-driven micromanipulator (MM33, Unisense, Århus Denmark). O_2 sensors were calibrated with fully oxygenated bottom water from the same station at ~1°C for saturation and for anoxic conditions by dissolving Na_2SO_3 in the same water. The first profile in each core was measured with a resolution of 1000µm as a quick scan to locate the sediment surface and to adjust the measuring range. Then the vertical resolution was increased to 100-500µm and additional five to seven profiles were measured at different points on the surface, approximately one cm apart from each other.

2.3. Whole-core sediment incubations

Four intact cores with clear overlying water were subsampled in the laboratory in acrylic tubes (i.d. 56 mm, height 25 cm) retaining about 10 cm of the overlying water. The sediment and water height in the tubes were approximately 10 cm. The cores were incubated in a 40-liter incubation tank filled with bottom water from the same station. Before the incubation the overlying water in the cores was equilibrated with bottom water in the tank.

The overlying water in the cores was stirred by small magnetic bars mounted in the core liners and driven by an external magnet at 60 rpm. The cores were pre-incubated uncapped for 6 hours and subsequently capped and incubated for a period of 6 to 24 hours depending on the initial oxygen concentration in the bottom water. 2D oxygen sensor spots (Firesting oxygen optode, PyroScience GmbH, Aachen, Germany) with a sensing surface of a diameter of 5 mm were attached to the inner wall of two incubation cores. The sensor spots were calibrated against O_2-saturated bottom water and oxygen-free water following the manufacturer's guidelines accounting for temperature and salinity of the incubation water. Measurements were performed with a fiberoptic cable connected to the spot adapter fixed at the outer core liner wall at the spot position. The O_2 concentration was continuously logged during incubations. Sediment total oxygen uptake (TOU) rates were computed by linear regression of the O_2 concentration over time. 5 ml of overlying water were removed over the course of the incubation used for nutrient and dissolved CO_2 analysis as described below. Linear regression best fits were used to determine the exchange fluxes of dissolved CO_2.

2.4. Extracted porewater analysis

Porewater samples for concentration measurements of total dissolved CO_2 (DIC), sulfate, and ammonium were obtained using the methods described in Seeberg-Elverfeldt et al. (2005). Rhizons were treated for 2 hours in 10% HCl solution, followed by two rinses with deionized water for 2 hours and final storage in deionized water. The rhizons were connected to 10 mL disposable plastic syringes with inert pistons (VWR, Stockholm, Sweden) via polyethylene 3-way luer-type stopcocks (Cole-Parmer, U.S.A.) and inserted in 1-cm intervals through tight-fitting, pre-drilled holes in the liner of the sediment cores. The first mL of pore water was discarded from the syringe. No more than 5 ml were collected from each core to prevent cross-contamination of adjacent porewater due to the suction effect (Seeberg-Elverfeldt et al., 2005). The collected porewater was divided into four different aliquots for later chemical analysis. For dissolved sulfate analysis, 1 ml of porewater was preserved with 200 µl of 5% zinc acetate solution and frozen. For ICP-AES analysis of dissolved metals and major cations, 1 ml of porewater was preserved with 100 µl of 10% Suprapur HNO_3 and stored cold. For analysis of dissolved ammonium, 2 ml of porewater were frozen untreated. For analysis of dissolved inorganic carbon, 2 ml of porewater were preserved with 100 µl 10% $HgCl_2$ and stored cold in brown glass vials without headspace. Ammonium was determined on a

QUAATRO 4-channel flow injection analyzer (Seal Analytical) on board. All other porewater analyses were performed at the Department of Geological Sciences, Stockholm University. Samples that were analyzed in the home laboratory remained cold or frozen on board until arrival of the icebreaker Oden in Sweden. Sulfate concentration was measured on diluted aliquots on a Dionex System IC 20 ion chromatograph. DIC concentrations were determined by flow injection analysis (Hall and Aller, 1992). Dissolved iron and manganese were determined on diluted aliquots by ICP-AES (Varian Vista AX). For carbon isotope analysis of dissolved inorganic carbon, 1 ml of porewater was filled into 12 ml exetainers to which 1 ml of concentrated phosphoric acid was added. The carbon isotope composition of the formed CO_2 was analyzed on a GasbenchII-MAT 253 isotope ratio mass spectrometer coupled to a GC-PAL autosampler. Results are reported in the conventional delta notation relative to PDB. Precision of isotope analysis is 0.1‰.

For the calculation of porewater concentration ratios of DIC and NH_4^+, the effects of different diffusion coefficients and ammonium adsorption were accounted for. We have no direct measurements of adsorption coefficients for these sediments. Instead, we used an ammonium adsorption coefficient of 1.3 established for comparable, terrestrially dominated silty clays in the East China Sea for which similar porosities and organic carbon concentrations were reported (Mackin and Aller, 1984). The diffusion coefficient of HCO_3^- is about 45% smaller than the diffusion coefficient of NH_4^+ (Li and Gregory, 1974). The two effects required an upward correction of the ammonium concentration by 40% to facilitate direct comparison in DIC/NH_4^+ ratios. Diffusion- and adsorption-adjusted DIC/NH_4^+ ratios were also corrected for the bottom water DIC and NH_4^+ concentrations (Table 1). Only concentrations below 4 cm depth were used for comparison to avoid effects of oxidation on NH_4^+ concentrations.

2.5. Reaction transport modelling

Reaction rates and fluxes were estimated from the concentration profiles of dissolved oxygen, manganese, iron, and dissolved inorganic carbon according to the general reaction-transport equation at steady state accounting for diffusion and advection exemplified here for dissolved oxygen according to

$$\frac{d}{dz} = \left(\varphi(D_s + D_b)\frac{dO_2}{dz}\right) + \varphi\alpha\left(O_{2,\ z=0} - O_{2,\ z}\right) + \sum R = 0 \quad (1)$$

At steady state, the rate of the concentration change reflects the balance between the consumption due to respiration and oxidation of reduced inorganic compounds (R) against diffusion and advection due to bioirrigation into sediment (Glud, 2008). D_s ($cm^2\ s^{-1}$) is the sediment diffusion coefficient and was calculated for the experimental temperature and salinity according to Boudreau (1997). The sediment diffusion coefficient D_s was recalculated from the molecular diffusion coefficient D_o according to $D_s = D_o / \theta^2$, where $\theta^2 = 1 - \ln(\varphi^2)$, where φ is porosity and θ is tortuosity (Boudreau, 1997). D_b ($cm^2\ s^{-1}$) is the bioturbation coefficient and α is the irrigation coefficient ($cm\ s^{-1}$). D_b and α were estimated by stepwise optimization by fitting a concentration profile to the measured data using the least square fitting procedure of the program Profile (Berg et al., 1998) testing various coefficients until the statistically best fit was obtained. Boundary conditions and the coefficients D_b and α for the best fits are shown in the supplemental material Table 1.

2.6. ^{35}S-Sulfate reduction rates

For the incubations, the whole-core incubation method by Jørgensen (1978) was used. $^{35}SO_4^{2-}$ tracer solution was diluted in a 6 ‰ NaCl solution containing 0.5 mM SO_4^{2-} and 2.5 µl of the tracer solution (200kBq) was injected through the pre-drilled holes. The cores were then capped and sealed in plastic wrap foil and incubated for 8 hours at the respective bottom water temperatures. After this time, the incubations were stopped by sectioning the core in 1-cm intervals to 5 cm depth and in two centimeter intervals below this depth to the bottom of the core. Sediment sections were transferred into 50 ml plastic centrifuge tubes containing 20 ml zinc acetate (20% v/v), mixed to a slurry on a vortex stirrer and frozen. The total amount of ^{35}S-labeled reduced inorganic sulfur (TRIS) was determined using the single-step cold chromium distillation method by Kallmeyer et al. (2004). TRIS and supernatant sulfate were counted on a TriCarb 2095 Perkin Elmer scintillation counter. The sulfate reduction rate was calculated using the following equation (Jørgensen, 1978):

$$^{35}SRR = \left(TRI^{35}S \times 1.045 \Big/ (^{35}SO_4^{2-} + TRI^{35}S) \right) \times [SO_4^{2-}]/\rho T \qquad (2)$$

where $[SO_4^{2-}]$ is the pore water sulfate concentration corrected for porosity ρ, $TRI^{35}S$ and $^{35}SO_4^{2-}$ are the measured counts (cpm) of sulfate and total reduced inorganic sulfur species, respectively, 1.045 is a correction factor accounting for the kinetic isotope effect of ^{35}S relative to ^{32}S, and T is the incubation time. The sulfate reduction rate is reported as nmol cm^{-}

^{3} day^{-1}. ^{35}SRR were measured in two parallel cores for all depth intervals. The incubation experiments were conducted between July 15 and August 20, but for logistical reasons (transport to Stockholm) the distillation of the samples was conducted between December 10, 2014 and April 2, 2015 so that between 1.7 and 2.7 half-lives of ^{35}S (87.4 days) had passed before all samples were processed. The resulting detection limit of the rate measurements accounting for distillation blanks and radioactive decay of ^{35}S between experiment and laboratory workup was 0.01 nmol cm^{-3} day^{-1}.

2.7. Carbon equivalent apportionment of terminal electron-accepting processes (TEAP)

The modelled oxygen, iron, manganese, and DIC reaction rates were integrated over a depth interval of 30 cm to permit comparison between different stations. The integrated terminal electron accepting process (TEAP) rates were recalculated into carbon equivalents for the electron acceptors oxygen, iron, manganese, and sulfate using an idealized $(CH_2O)_x$ stoichiometry for organic matter (Vandieken et al., 2006; Nickel et al., 2008). The contribution of inorganic reoxidation to oxygen consumption and the effects of internal recycling of sulfur, iron, and manganese are discussed in section 4.1. The calculated rates were then used to calculate the contribution of the different aerobic and anaerobic electron acceptors to total carbon mineralization for 5 stations in the Laptev and East Siberian Sea (Table 3).

2.8 Marine versus terrestrial endmember partitioning of carbon degradation rates

In order to determine the mineralized proportion of terrestrial and marine organic matter in the sediment directly, the DIC concentrations and the carbon isotope composition of DIC were used as indicators of remineralized organic matter in the sediment. The remineralized fraction (F) of $DIC_{total,\ depth\ x}$ at the different sediment depths (x) was defined as

$$F = (DIC_{total,\ depth\ x} - DIC_{bottom\ water\ overlying\ core})/DIC_{total,\ depth\ x} \quad (3)$$

and this fraction was plotted against the respective carbon isotope composition of $DIC_{total,\ depth\ x}$ (Fig. 6B). The y-intercept of the linear regression was constrained by the carbon isotope composition of DIC in the bottom water for the respective station so that the slope of the regression line was the only unknown in this analysis. The gradients for each station yielded

the average stable carbon isotope composition of the remineralized organic matter in the sediment assuming no or very minor isotope fractionation during the oxidation of organic matter. This calculation assumed that porewater removal or addition of DIC by diagenetic processes such as $CaCO_3$ precipitation or dissolution was minor and time-invariant, which is supported by the observation that Ca^{2+} and Mg^{2+} porewater concentrations at these shelf and slope stations did not change significantly with depth (Brüchert and Sun, unpubl. data). The relative contributions of the terrestrial and marine organic carbon were then calculated with a linear two-endmember isotope model:

$$\delta^{13}C_{DIC,\ remineralized} = f_{terr} * \delta^{13}C_{terr\ OC} + f_{mar} * \delta^{13}C_{marine\ OC} \quad (4)$$

where f_{terr} and f_{mar} are the respective mass fractions of terrestrial and marine-derived organic carbon and $\delta^{13}C_{terrestrial}$ and $\delta^{13}C_{marine}$ reflect the isotope composition of these endmembers. In order to derive specific degradation rates of the marine and terrestrial carbon fractions, the endmember mixing-based assessment of the marine and terrestrial organic carbon contributions to DIC were combined with the mineralization rates derived for the different electron acceptors.

3. Results

3.1. Physical and chemical bottom water conditions

Table 1 summarizes the general site characteristics of the investigated sediment stations. Bottom water salinity varied between 34.9 ‰ in the outer Laptev Sea at 3146 m depth (Station 1) to 29.1 ‰ in the East Siberian Sea at 40 m (Station 45). The lower salinity in the East Siberian Sea can be attributed to longshore transport of freshwater eastward from the Lena River. Bottom water temperatures varied between -1.8°C at Station 27 and 0°C at Station 37, but there was no regional trend in the data. Cored sediment consisted of silty clays to clayey silts. Slope sediment had a distinctly brown color throughout the cored interval, whereas shelf sediment only had a 1 to 4 cm-thick brown interval, below which the sediment color changed to grey. In the eastern part of the East Siberian Sea, the sediment was mottled black below 10 cm depth. Iron-manganese concretions were found between 2 cm and 10 cm depth at stations 24, 42, and 43, but were also observed at other stations on the shelf that were not part of this study. Benthic macrofauna, when present, consisted mainly of brittle stars, isopods, few polychaetes, and rare bivalves. All bottom waters were well-oxygenated with

concentrations higher than 190 µmol/l, but the shelf bottom-waters in the East Siberian Sea had generally lower concentrations than in the Laptev Sea and bottom waters on the continental slope had lower oxygen concentrations than on the shelf. Concentrations of bottom-water ammonium ranged between 0.2 µmol/L and 1.8 µmol/L. Generally, the slope stations and the shelf stations nearest to the Lena delta had the highest ammonium concentrations, whereas the other shelf stations showed no clear regional trend other than proximity to the Lena delta. Bottom water dissolved inorganic carbon concentrations varied between 2086 µM (Station 53) and 2598 µM (Station 27), and the stable carbon isotope composition of DIC in the waters overlying the cores were between -0.5 ‰ and -6.5 ‰ vs. VPDB.

3.2. Dissolved oxygen, manganese, and iron

We show representative profiles of oxygen concentrations in Figure 2 for the Laptev Sea slope station 1, the Laptev Sea shelf stations 23, 30, 45, and the East Siberian Shelf Sea 53 and 63. Oxygen penetration depths varied between 3 mm at Station 58 and more than 60 mm in all slope sediments (Table 2). For the Laptev Sea slope stations 1, 2, 3, and 4, the maximum depth of oxygen penetration could not be determined, because at penetration greater than 60 mm the conical sensor needle opened a hole in the sediment through which oxygen-containing bottom water could potentially have entered the sediment at depth thereby artificially extending the oxygen penetration depth. In the slope-to-shelf transects the oxygen penetration depth decreased from >60 mm off-shore to 10 mm at the most inshore station in the Laptev Sea and the East Siberian Sea. At the two easternmost shelf stations 58 and 63, we measured the lowest oxygen penetrations depths, 3 mm and 4 mm, respectively. Evidence for bioturbation and bioirrigation based on multiple microelectrode profile measurements per core was rare. Only at Station 48 a clear increase in oxygen concentrations below the sediment surface was observed, indicative of active bioirrigating macrofauna. However, even at this station, based on investigations in parallel multicore casts, fauna was not abundant (A. Gukov, pers. comm.). At all other stations, oxygen concentrations decreased exponentially with depth. Fitting of the oxygen concentration profiles to the steady advection-diffusion-transport model (Eq. 1) yielded fluxes that varied between 0.81 and 11.49 mmol m^{-2} d^{-1} (Table 2). These calculated O_2 fluxes compared well with total oxygen uptake rates calculated from whole-core incubations using 2D optode sensor spots (Table 2). The good fit between

the two methods also supports the notion that bioirrigation and bioturbation effects from meiofauna and macrofauna were minor.

In the slope sediment at Station 1, concentrations of dissolved manganese and iron were low throughout the cored depth interval and below 0.2 and 0.5 µM, respectively. The exception was a small increase for both elements between 4 and 8 cm depth and 14 and 20 cm depth to concentrations of less than 3 µM, possibly due to slightly more degradable organic material in these depth intervals (Fig. 2). A similar concentration profile was found for the other slope station 4 (data not shown), but here concentrations were below 2 µM throughout for both dissolved iron and manganese and only slightly higher in the topmost cm. On the shelf, in the Laptev Sea (Station 23 and 30), concentrations of dissolved manganese and iron were below 0.3 µM and 1.5 µM, respectively, in the top 2 cm and 3 cm at Station 23, before increasing to maximum concentrations of 69 and 134 µM. At both stations, metal concentrations decreased again below the concentration maximum indicating that deeper buried sediment was not a source of the metals and that the dominant source of iron and manganese was reduction in the topmost 5 cm of sediment. There was a general trend of increasing manganese concentrations from west to the east. At Station 30 in the Laptev Sea, the concentration of dissolved manganese was less than 0.3 µM in the topmost cm, but increased steeply before increasing to maximum concentrations of 189 µM at 9 cm depth. Similarly, dissolved iron concentrations were below 1 µM to 4 cm depth and then increased to 144 µM. Again, below the maximum, both iron and manganese porewater concentrations decreased with increasing sediment depth. Even higher iron and manganese concentrations were found in the East Siberian Sea (Stations 45, 53, 63), where dissolved manganese already increased from the bottom water to concentrations of 20 µM in the topmost centimeter of sediment, and iron increased to above 1 µM below 2 cm depth. The steepest manganese concentration gradient was found at Station 63 in the easternmost East Siberian Sea, where concentrations were 501 µM in the first cm of sediment with a concentration maximum of 548 µM at 2.5 cm depth and decreasing below this depth to 115 µM at 30 cm depth. Station 63 differed with respect to dissolved iron concentrations from the other stations, because here dissolved iron showed two small peaks at 3.5 cm and 7 cm, and concentration increased substantially only below 17 cm depth to concentrations of 189 µM.

3.3. ^{35}S-sulfate reduction rates and porewater sulfate

Sulfate concentrations showed minor depth gradients at all sampling sites (Fig. 3) and decreased from starting concentrations between 23.9 mM and 28.1 mM by 0.4 mM to 2.5 mM from the top to the bottom of the cores. At all stations, turnover of ^{35}S-tracer was recorded from the topmost sediment interval to the bottom of the core indicating active bacterial sulfate reduction (Fig. 3). Depth-integrated rates over the recovered core lengths varied between 0.03 and 1.41 mmol m^{-2} d^{-1} (Table 2). The integrated rates were lowest at Station 1 at 3146 m in the Laptev Sea and highest at the Station 63 in the easternmost East Siberian Sea. Across the shelf (Stations 6 to 24), depth-integrated rates increased from the west to the east. Example depth profiles of depth-specific sulfate reduction rates are shown in Fig. 3 for the same six stations as previously. At Station 1, these rates ranged from 0.03 to 0.38 nmol cm^{-3} d^{-1}. At this station, the variability between replicate cores was large, which is attributed to the fact that many rates were near the detection limit in our handling procedure. Overall, sulfate reduction was higher in the top 10 cm of sediment, but showed no pronounced change with depth at this station. This suggests that the reactivity of the organic material did not change substantially over the cored depth interval. The second slope station, Station 4, showed a similar rate-depth profile than Station 1. Depth profiles for the mid-outer shelf stations 23 to 63 all showed broad sub-surface maxima between 2.5 and 17.5 cm, but the depths of the rate maxima differed between the different stations (Fig. 3). Peak rates varied between 0.6 nmol cm^{-3} d^{-1} at Station 30 and 39 nmol cm^{-3} d^{-1} at Station 63. The second highest rate, 7.6 nmol cm^{-3} d^{-1}, was found at the station nearest to the Lena delta, Station 23. At all stations, sulfate reduction rates decreased from the maxima to rates below 1 nmol cm^{-3} d^{-1} or to below the detection limit at the bottom of the cores. A particularly sharp decrease in the sulfate reduction rate was observed between 8 and 9 cm at Station 63, where rates dropped from 8.5 to 0.1 nmol cm^{-3} day^{-1} over 1 cm depth. Since sulfate was abundant throughout the cored intervals, this order-of-magnitude decrease indicates substantial changes in the reactivity of buried organic matter. Although no abrupt change in grain size or organic carbon was observed in this core, it is likely that a historical change in organic sedimentation took place during deposition across this time interval.

3.4. Porewater dissolved inorganic carbon (DIC), ammonium (NH_4^+), and $\delta^{13}C_{DIC}$

Porewater concentrations of dissolved inorganic carbon (DIC) and ammonium (NH_4^+) increased with depth at all stations (Fig. 4). The increase of DIC was between 0.6 mM

914 (Station 23) and 2.3 mM (Station 45) over the cored sediment depths and ammonium
915 concentrations increased between 16.8 µM (Station 1) and 549 µM (Station 50). The
916 steepness of the depth gradients was consistent with the rates of oxygen uptake and bacterial
917 sulfate reduction for the different stations. The porewater pattern at Station 63 is an exception,
918 because this station had the highest oxygen uptake and the highest sulfate reduction rates of
919 all stations, but showed only a modest increase in DIC and NH_4^+ concentrations by 1.5 mM
920 and 57 µM, respectively, over the cored sediment depth. This apparent discrepancy can be
921 explained by the very low rates of sulfate reduction below 10 cm depth. Since these deeper
922 layers have not produced large amounts of DIC and NH_4^+, only the surface 10 cm contribute
923 significantly to total carbon mineralization and ammonium production.

924 For the anoxic parts of the sediment, DIC/NH_4^+ ratios varied between 8.4 for Station 24 and
925 53 and 58, respectively for Stations 1 and 4 in the Laptev Sea, and between 7.2 and 18.8 in the
926 East Siberian Sea, with an overall mean DIC/NH_4 ratio of 9.8 for all stations excluding the
927 continental slope stations. The $\delta^{13}C$ values of DIC consistently decreased with sediment depth
928 indicating the addition of ^{13}C-depleted remineralized carbon to DIC. The greatest downcore
929 depletion in ^{13}C was observed at Stations 45, 48, and 50, where $\delta^{13}C$ of DIC decreased from -
930 2.0 ‰ near the sediment surface to -13.9, -16.4, and -18.6 ‰ at the bottom of the cores (Fig.
931 4).

932

933 **3.5. Modelled oxygen, iron, and manganese reduction rates**

934 Results of the reaction transport modelling of dissolved oxygen, iron, and manganese
935 concentration profiles for Station 23 are shown in Fig. 5. O_2 consumption rates exceeded
936 sulfate, iron, and manganese reduction rates by a factor of more than 100 (Fig. 5). For the
937 shelf stations, most of the carbon oxidation therefore takes place in the topmost 5 mm. The
938 reaction rate profiles for iron and manganese reduction indicate that manganese reduction
939 dominates in the topmost 2 cm of sediment followed by co-existing iron and sulfate reduction
940 below (Fig. 5). These observations are consistent with results from the northern Barents Sea
941 by Vandieken et al. (2006) and Nickel et al. (2008). Optimal fits of the concentration profiles
942 required a bioirrigation coefficient of 1×10^{-4} cm^2 sec^{-1} in the topmost 2 cm of sediment at
943 Stations 23 and 53. For the other stations, optimal fits required no sediment mixing by
944 bioturbation or advective porewater transport by bioirrigation. This result is consistent with
945 the modelling results of the oxygen microelectrode profiles and the low numbers of

946 bioturbating macrofauna in the outer shelf sediment. Bacterial sulfate reduction was detected
947 already at a depth where the sediment was still brown indicating abundant iron
948 oxyhydroxides. It is therefore likely that the modelled negative iron production rates at the
949 sediment surface indicate iron oxidation in the mixed upper layer. This pattern was not
950 observed for manganese, which is consistent with incomplete manganese oxidation at the
951 sediment surface and loss of dissolved manganese to the bottom water. Manganese and iron
952 reduction contributed between 2.3 and 23.7% to the total anaerobic carbon mineralization and
953 between 0.3 and 2.3% to the total carbon mineralization (Table 3). Although these numbers
954 may somewhat underestimate the contribution of metals to carbon mineralization , our results
955 indicate that bacterial sulfate reduction is by far the major anaerobic carbon mineralization
956 pathway in these sediments.

957

958 **4. Discussion**

959 **4.1. The relative importance of iron, manganese and sulfate reduction for carbon**
960 **degradation**

961 There was a statistically significant positive correlation between the dissolved oxygen
962 uptake and anaerobic carbon degradation rates by sulfate reduction with an r^2 of 0.72 ($P < 0.05$).
963 This reflects the coupling of oxygen uptake to the oxidation of reduced inorganic
964 metabolites (FeS and H_2S) produced during the anaerobic metabolism by sulfate reduction
965 (e.g., Glud, 2008; Jørgensen and Kasten, 2006; Thamdrup, 2000; Berg et al., 2003) (Fig. 9).
966 The slope of the regression line for the data set is 6.1±1.1 indicating that about 16.4% of the
967 oxygen uptake is used for the oxidation of reduced manganese, ammonium, dissolved iron,
968 and iron sulfides and elemental sulfur. This amount is slightly lower than the average 23%
969 estimated for oxygenated coastal and continental shelf sediment (Canfield et al., 2005), but is
970 consistent with the notion that a substantial amount of the buried organic matter in Siberian
971 shelf sediment is oxidized anaerobically. The lower proportion of anaerobic respiration to
972 aerobic respiration compared to other shelf environments likely reflects the greater proportion
973 of highly reactive marine-derived organic material in the topmost millimeters of sediment.

974 The prevalence of bacterial sulfate reduction in anaerobic carbon mineralization agrees with
975 the assessment made by Vandieken et al. (2006) and Nickel et al. (2008), who suggested that

more ice-free stations in the northern Barents Sea supported higher rates of sulfate reduction than the more permanently ice-covered stations reflecting lower carbon export production.

The efflux of manganese to the bottom water on the eastern Siberian shelf supports the assessment by Macdonald and Gobeil (2012) that Arctic shelves can export dissolved manganese to the Arctic interior. Coexistence of net iron reduction and sulfate reduction at the same depths make it difficult to quantify how much of the iron reduction is coupled to heterotrophic carbon oxidation and to the re-oxidation of sulfide produced from bacterial sulfate reduction. Qualitatively, the presence of dissolved iron throughout the measured porewater profile implies that iron reduction exceeded concomitant sulfate reduction, iron sulfide precipitation, and reoxidation reactions, which supports the assessment of net heterotrophic iron reduction. However, previous investigations of the importance of iron and manganese reduction in Arctic shelf sediments have emphasized the importance of directly coupled redox processes between iron and manganese (Vandieken et al., 2006). It is also important to note that iron and manganese oxyhydroxides can sorb Mn^{2+} and Fe^{2+} (Canfield et al. 1993). The concentrations of dissolved Fe^{2+} and Mn^{2+} may therefore underestimate the actual concentrations of the reduced forms in these sediments.

Iron hydroxide surfaces have been inferred as important mineral surfaces for the preservation of organic matter (Lalonde et al., 2012; Salvado et al., 2016). In all cases studied here, the integrated net DIC production based on the porewater gradient of DIC, and the depth profiles of iron reduction indicate co-existing heterotrophic and chemical iron reduction and bacterial sulfate reduction. In addition, the porewater modelling results suggest that bioturbation can be an important sediment mixing process only for some shelf stations. Organic matter sorbed to mineral surfaces with deposition would thus have been subject to repeated desorption as iron oxyhydroxides were reduced. While this observation does not contradict the observation that some organic material is buried in association with iron oxyhydroxides, the repeated redox cycling of the oxyhydroxides would prevent the sorptive preservation of organic compounds.

4.1. Marine versus terrestrial organic matter contribution

Terrestrial organic carbon sources to the Laptev and East Siberian shelf and slope are riverine discharge and coastal erosion of the ice core complex (Stein and Macdonald, 2004;

Vonk et al., 2012; Rachold et al., 2004; Fahl and Nöthig, 2007; Semiletov, 1999). Marine organic carbon is derived from open-water production during the ice-free months, export of ice algae, and new production in polynyas (Sakshaug et al., 2004; Nitishinsky et al. (2007). Generally, marine productivity in the Laptev Sea is low and controlled by the nutrient concentrations derived from Atlantic water, but spring outflow from the Lena River provides an additional temporary land-derived nutrient source (Pivovarov et al., 1999; Sakshaug et al., 2004; Nitishinsky et al., 2007; Bourgeois et al., 2017) during late spring ice melt (Raymond et al., 2007). Terrestrial-derived nutrients can also affect marine productivity either directly by new production, or indirectly, due to plankton production from remineralized terrestrial DOC/POC (Alling et al., 2012). In the eastern East Siberian and Chukchi Sea, the inflow of nutrient-rich Pacific water supports higher marine primary productivity (e.g., Grebmeier et al., 2006). Ice-rafted transport and bottom boundary layer transport are the two most important modes of particle transport (Wegner et al., 2005; Bauch et al., 2009). Since all sediments sampled in this study were fine-grained siltey clays and clayey silts, coarse-grained woody, ice-rafted material played only a minor role for deposition of organic matter on the outer shelf and slope sediment. The transport direction of inner shelf sediments has been suggested to follow the predominant atmospheric regime, which is thought to be linked to the Arctic Oscillation (AO) (Dimitrenko et al., 2008; Guay et al., 2001; Weingartner et al., 1999). During positive AO southwesterly winds lead to generally eastward transport and repeated inshore transport in the BBL, whereas negative AO favors southerly winds and a predominantly northward transport (Guay et al., 2001; Dmitrenko et al., 2008). Offshore transport of dissolved and particulate organic matter from the Lean delta to the north can occur with the Transpolar Drift, but terrestrial organic material is also transported eastward and obliquely offshore with the Siberian coastal current receiving additional organic material from the Indigirka and Kolyma rivers (Guo et al., 2007; Dudarev et al., 2006). East of 140ºE, the influence of Pacific-derived nutrient-rich water supporting marine production is stronger the further east and offshore the sampling stations are located (Semiletov et al., 2005) (Fig. 1).

Carbon degradation rates in the sediment across the whole Siberian shelf and slope reflect this temporally and spatially diverse distribution of nutrient availability, ice cover, sediment deposition, and current flow regime (Rachold et al., 2004; Dudarev et al., 2006; Semiletov et al., 2005; Sakshaug et al., 2004; Dmitrenko et al., 2005). The proportion of degradable marine-derived organic material at the eastern Stations 50 to 63 on the East Siberian shelf is higher than at the western stations in the Laptev Sea, in line with higher

nutrient availability due to the Pacific influence. Ice-free conditions and the opening of water due to northward migration of ice shortly before the sampling likely supported new algal primary production at the shelf stations closest to land leading to enhanced export and deposition on the seafloor. During the time of sampling, only Stations 6 to 27 were ice-free, while Stations 23 and 24 had the longest ice-free condition before sampling. By contrast, Stations 30 to 63 were still covered by ice during sampling. New export of reactive organic material explains why O_2 uptake rates were the highest at stations 23 and 24 along the shelf to slope transect from station 1 to station 24 (Boetius and Damm, 1998). The same pattern as for the O_2 uptake rates is also observed for the sulfate reduction rates indicating that reactive organic matter is also buried below the oxygen penetration depth and mixed layer into the sulfate-reducing zone. This indicates that a greater portion of reactive organic material is buried closer to the Lena delta.

Published organic carbon budgets for the Arctic shelves infer an average burial efficiency of about 1% of exported marine OC (Stein and Macdonald, 2004), while terrestrial organic carbon, only accounting for about 10% of the organic carbon delivered to the Arctic Ocean bottom, has been suggested to be preserved with about 90% efficiency (Macdonald et al., 2015). Recently, Semiletov et al. (2016) compiled a large dataset indicating substantial aragonite undersaturation of Arctic shelf bottom waters from the Laptev, the East Siberian, and the Russian part of the Chukchi Sea, which was interpreted due to the remineralization of terrestrial organic matter. The observation of strongest aragonite undersaturation in the bottom waters supports a sediment-derived CO_2 source or a stagnant bottom boundary layer (Semiletov et al., 2013). It is therefore possible that oxic carbon mineralization in the topmost mm of sediment is a major CO_2 source for the overlying water.

Fig. 6 shows exemplary gradients of the regression for the six stations presented before and Table 4 lists the derived carbon isotope compositions of remineralized organic matter for all stations. The range of $\delta^{13}C$ of remineralized DIC varied between -18.8 ‰ ± 1.1 ‰ (Station 53) and -35.8‰ ± 3.0 ‰ (Station 1). The strongly ^{13}C-depleted isotope composition of -35.8 ‰ for remineralized DIC at Station 1 suggests the mineralization of strongly ^{13}C-depleted organic matter and possibly a strong contribution of terrestrial organic matter to carbon mineralization far offshore, in line with the very high DIC/NH_4^+ ratio of the porewaters at the slope stations. The potential existence of degradable terrestrial organic matter in slope sediments of 3000 m water depth is intriguing, since it would imply downslope transport and degradation of terrestrial organic matter. Northward off-shelf transport of terrestrial organic

matter with the Transpolar Drift is a viable transport mechanism. The contribution of degradable terrestrial organic matter to DIC in lower slope sediments is also supported by the observation of terrestrially derived biomarkers in porewater DOC of central Arctic Ocean sediment analyzed by FT-ICRMS (Rossel et al., 2016) and deep-water sediment trap data in the central Arctic Ocean (Fahl and Nöthig, 2007), but requires further investigation.

The isotope composition of the remineralized DIC therefore reflects mineralization of a mixture of organic molecules of different origins – interpreted here as a mixture of terrestrial and marine-derived organic matter. For the following discussion, given the uncertainty of the organic matter origin in slope sediment, we exclude data from the slope stations and restrict the discussion to the use of the following end member compositions for the shelf stations. For the Laptev Sea shelf, we account for the fact that a fraction of the DIC used for marine production is derived from remineralized terrestrial DOC and POC in shelf waters. Alling et al. (2012) report $\delta^{13}C_{DIC}$ values for offshore DIC samples below the halocline varying between -2 and -4 ‰. We therefore use an isotope endmember for marine organic matter of -24 ‰ and an isotope composition of -28 ‰ for the terrestrial organic carbon contribution (Alling et al., 2010; Vonk et al., 2012). For the East Siberian Sea East of 140°E, the heaviest calculated isotope composition of remineralized DIC was -19 ‰ and is used here as the marine endmember (Station 53). The same carbon isotope composition of -28 ‰ as for the Laptev Sea was used as the terrestrial end member. The heavier marine $\delta^{13}C$ value in the East Siberian Sea is supported by the slightly heavier $\delta^{13}C_{DIC}$ values reported for the offshore East Siberian Sea, which vary between 0 and -2 ‰ (Alling et al., 2012).

The calculated mass fractions of the two endmembers are listed in Table 4. Based on this analysis the porewaters on the Laptev Sea shelf contain a significant proportion of terrestrially derived organic matter, comprising on average 36 % of the remineralized DIC. This proportion decreases to average values of 32% in the East Siberian Sea, in line with a greater marine production in this area due to the inflow of Pacific water (Semiletov et al., 2005, Dudarev et al., 2006; Naidu et al., 2000).

Since ^{35}S-sulfate reduction rates comprise most of the anaerobic carbon mineralization of sediment buried below the oxygen penetration depth, our assessment includes, in contrast to earlier studies, the mineralization rates of terrestrial organic matter beyond the short time period of oxygen exposure in the topmost mm of sediment. Using sedimentation rates of 0.8 mm y^{-1} for the outer Laptev Sea (Strobl et al., 1988) and 1.4 mm y^{-1} for the outer East

Siberian Sea (Bröder et al., 2016b), the recovered sediments record a time interval of 250 to 700 years since burial. Using the mass fractions of terrestrial and marine-derived organic carbon listed in Table 4, respective mineralization rates of the terrestrial and marine carbon fractions were calculated from the product of the mass fractions and the depth-integrated ^{35}S-sulfate reduction rates (Table 2). This approach is only applicable in combination with depth-integrated anaerobic carbon mineralization rates, but would be biased if used in combination with total oxygen uptake rates. The reason for this is that the depth of oxygen penetration varied only between a few millimeters to little more than a centimeter on the shelf, whereas the corresponding DIC concentrations, even in the topmost centimeter of sediment, are affected by diffusive exchange along the 30 cm-long concentration profile smoothing out depth-dependent changes in the source signal of organic matter. It is therefore not possible to assess the relative fractions of terrestrial and marine organic matter mineralized for discrete depth intervals. Our combined radiotracer and DIC stable isotope approach suggests that both marine and terrestrial organic matter are degraded in the buried sediment and that both pools contribute to degradation products in anoxic buried sediment. This assessment is a significant modification to earlier studies by Boetius and Damm (1998) and Bourgeois et al. (2017), who have described organic matter mineralization in Siberian Arctic sediments largely as a function of oxygen uptake.

Carbon mineralization rates measured along the transect near 130ºE (Stations 1 through 24) reflect the influence of gradual offshore transport of terrestrial organic material (Bröder et al., 2016a) (Fig. 7A, B). A comparison with the oxygen uptake rates reported by Boetius and Damm (1998) indicates that all rates measured in 2014 were significantly higher than the rates measured in 1993 by Boetius and Damm (1998). Although the different rates may reflect a seasonal effect since Boetius and Damm's data were acquired later in the year than our data, the increase may also point to higher organic carbon mass accumulation rates compared to 20 years ago, consistent with a decrease in the annual ice cover over the past 20 years in the Arctic (Arrigo and van Dijken, 2011; Stroeve et al., 2012; Walsh et al., 2017). Whether these rates reflect higher marine and/or terrestrial accumulation cannot be answered satisfyingly with this data set.

Fig. 8A compares the oxygen uptake rate of the stations of this study with averaged oxygen uptake rates from the literature for different shelf, slope, and abyssal plain environments worldwide (Canfield et al., 2005). The data suggest that there is no significant difference in the oxygen consumption rates between the Siberian shelf and slope and other

continental margin environments. ^{35}S-sulfate reduction rates in Sea Siberian slope sediment are also comparable rates to those in other slope environments (Fig.7B and 8B), but the sulfate reduction on the shelf are lower by a factor up to 15. Another difference apparent from this comparison is the similarity in sulfate reduction rates for the outer shelf and continental slope sediments of the Siberian Arctic (Fig. 8B). This similarity is noteworthy for several reasons: 1) it suggests that the kinetics of anaerobic carbon degradation in the shelf and slope sediments reflect similar reactivity of the organic matter. This is surprising since accumulation rates on the continental slope are significantly slower than on the outer shelf. 2) The absolute magnitude of the sulfate reduction rates in shelf and slope sediment indicate significant rates of organic matter mineralization long after burial consistent with the substantial DIC flux and the strongly ^{13}C-depleted DIC carbon isotope composition. Overall, the data indicate that organic matter reactivity substantially changes during burial in shelf sediment, but that the reactivity of transported organic matter that is exported to deep water across the shelf does not decrease significantly supporting long-term slow mineralization rates in the slope environment. Accumulation of the organic material on the slope may therefore be related to rapid downslope transport of organic material or a rapid offshore transport, e.g., due to transport with ice or as bottom nepheloid layers cascading from the shelf edge (Ivanov and Golovin, 2007).

4.2. Assessment of carbon burial efficiency

Reported ^{210}Pb-based sediment accumulation rates in outer Siberian shelf sediment range between 0.05±0.02 g cm^{-2} y^{-1} in the Laptev Sea (Strobl et al., 1988) and 0.24±0.04 g cm^{-2} y^{-1} in the East Siberian Sea (Bröder et al., 2016b). Given surface sediment organic carbon concentration for this area between 1% and 1.5%, the resulting organic carbon mass accumulation rates vary between 1.1 mmol m^{-2} d^{-1} and 1.7 mmol m^{-2} d^{-1} for the Laptev Sea (area near Station 23) and 5.5 and 8.2 mmol m^{-2} d^{-1} in the East Siberian Sea (data for Station 63). We estimated the burial efficiency of terrestrial organic carbon from the ratio of the depth-integrated sulfate reduction rates relative to the ^{210}Pb mass accumulation rate of organic carbon. This treatment assumes that the reported organic carbon mass accumulation rates largely reflect the refractory component of organic matter. While it is possible that a fraction of terrestrial and marine organic matter is degraded on shorter time scales than captured by the ^{210}Pb method, we assume that the fraction of highly reactive terrestrial organic matter

missed in this treatment is small. The resulting burial efficiency of the terrestrial carbon fraction is on average 91 ± 6 % in the Laptev Sea and 94 ± 4 % for the East Siberian Sea. We also calculated apparent degradation rate constants of organic matter assuming first order degradation kinetics for the time duration of sediment burial recorded in the sediment cores. For this assessment, we used the total depth-integrated anaerobic carbon mineralization determined from the combined manganese, iron, and sulfate reduction rates for the recovered sediment. The apparent annual degradation rate constant (k) was then calculated from

$$k_{terrestrial} = \frac{\left(-ln\frac{\int_0^{30} OC_{accumulation} - \int_0^{30} OC_{total\ mineralization}}{\int_0^{30} OC_{accumulation}}\right)}{t_{burial}} \quad (5)$$

where the integrals of $OC_{accumulation}$ and $OC_{mineralization}$ cover a period of 250 years to 700 years based on the ^{210}Pb mass accumulation rates. The resulting annual degradation rate constant ($k_{terrestrial}$) ranges between 1 x 10^{-4} y^{-1} and 5 x 10^{-4} y^{-1} averaging 1.5 x 10^{-4} y^{-1} in the Laptev Sea and between 8 x 10^{-5} and 3 x 10^{-4} y^{-1} averaging 1.2 x 10^{-4} y^{-1} in the East Siberian Sea.

A comparison of the total oxygen uptake with the C_{org} mass accumulation rates indicates that the ^{210}Pb-based C_{org} mass accumulation rates on the shelf are equal or significantly lower than the oxygen uptake rates, with a discrepancy of up to a factor 10. Since the derivation of the ^{210}Pb-based C_{org} mass accumulation rates is based on the same depth range as our direct ^{35}S-based degradation rate measurements (30 cm of sediment, Vonk et al., 2012), C_{org} mass accumulation rates and degradation rate measurements cover the same time window of sediment burial. Temporal variation in sediment accumulation therefore cannot explain the discrepancy. In addition, methane seep sediments where upward transport of methane from deeper sediment layers contributed to oxygen uptake were excluded from this data set. The best explanation for the discrepancy is therefore that the ^{210}Pb-mass accumulation rates underestimate the true mass accumulation rate of highly reactive organic material and that this material is oxidized at the sediment surface. Based on the measured oxygen uptake rates this freshly deposited organic material has substantially higher degradation rates within the top mm of sediment as reflected by the steep O_2 gradients. ^{210}Pb-based organic carbon accumulation therefore reflects the long-term burial of less reactive organic material in the top 30 cm of sediment. Since anaerobic degradation processes prevail below the O_2 penetration depth, the measured burial efficiency of the accumulating organic material is therefore a function of the anaerobic bacterial degradation rather than the aerobic degradation efficiency. This conclusion has implications regarding the assessment of potential

aerobic degradation of reactive terrestrial organic matter, since degradation of such material would have gone undetected with ^{210}Pb-based accumulation rate measurements.

4.5. Regional estimates

We present areal estimates of sediment carbon mineralization by extrapolating the measured carbon mineralization rates over the outer Laptev Sea and East Siberian Sea shelf. Such extrapolations of benthic carbon mineralization rates are notoriously difficult given sediment heterogeneity and insufficient temporal data coverage of benthic carbon mineralization rates. For this investigation, no near-shore or slope stations were included in the assessment. The near-shore Siberian shelf environments are under much stronger influence by coastal erosion and riverine discharge than the outer shelf stations and have considerable longer open-water conditions than the outer shelf stations investigated here. In addition, the sedimentation pattern in the near-shore environments is significantly more diverse, which will affect sedimentation rates, grain size distribution, and carbon contents. For this reason, we did not extend our extrapolations to the inner shelf environments. Some of these inner shelf settings likely have much higher benthic carbon mineralization rates and additional studies are required to constrain these better. Our coverage of the slope stations is insufficient for meaningful spatial extrapolations. A large data set for this region has been analyzed by Miller et al. (2016) and the reader is referred to this work.

We estimate the extent of the outer shelf area with depositional conditions comparable to those investigated here to cover approximately 280,000 km^2 of the Laptev Sea. For the East Siberian Sea, we estimate the respective area of the outer shelf to be 340,000 km^2. Due to the stronger terrestrial influence in the Laptev Sea, we calculated rates separately for the two shelf seas. The areal coverage with sediment stations was too sparse for statistically significant interpolations between stations that would give reliable spatial accounts of the gradients in rates between the stations. Instead, arithmetic averages of sediment mineralization rates and fluxes were calculated for these regions. Accepting the uncertainties in our assessment and data density, we estimate that the calculated areal rates could deviate by up to 50%. Table 5 lists the calculated rates based on the average flux calculated per square meter per day for oxygen uptake, DIC flux, bacterial sulfate, and total anaerobic carbon mineralization. For the

latter three methods, the total flux was calculated for the marine and terrestrial component, respectively. The same analysis cannot be performed for the oxygen uptake for the reasons discussed in section 4.3. Since the major part of the oxygen uptake is likely associated with degradation of a highly reactive marine organic carbon component, the proportions calculated based on the $\delta^{13}C$ composition of DIC would not necessarily apply to the topmost mm of sediment. It is noteworthy to say that the rates calculated with our data set agree well with the O_2 uptake rates recently published by Bourgeois et al. (2017) for the Laptev Sea. Our calculations suggest that 5.2 and 10.4 Tg O_2 y^{-1}, respectively are taken up by the outer shelf sediment in the Laptev and East Siberian Sea, respectively, totaling 15.9 Tg y^{-1} for the whole investigated area (Table 5). Anaerobic carbon mineralization based on DIC, ^{35}S-SRR and combined manganese, iron, and sulfate reduction range between 0.62 and 1.28 Tg y^{-1}. Of the total anaerobic carbon mineralization, between 0.25 and 0.48 Tg y^{-1} can be attributed to the oxidation of terrestrially derived organic material. This rate is five to ten times lower than the estimated annual water column degradation of particulate terrestrial organic matter in the Eastern Siberian Arctic shelf system of 2.5±1.6 Tg y^{-1} (Sanchez et al. 2011), and only between 0.5% and 2% of the annual organic carbon export from land (Stein and Macdonald, 2004; Vonk et al., 2012).

5. Conclusions

Directly measured carbon mineralization rates together with stable isotope and concentration data of East Siberian Arctic shelf and slope porewaters indicate that about one third of the remineralized organic carbon in porewater DIC is derived from terrestrial organic matter. This conclusion confirms and extends previous observations that terrestrial organic carbon buried in Siberian shelf and slope sediment is not conservative (Semiletov et al., 2013; Karlsson et al., 2015; Bröder et al., 2016b). While mineralization of terrestrial organic material has been described for the water column and resuspended surface sediment, our data indicate that mineralization also proceeds long after burial in sediment. The estimated apparent carbon degradation rate constants of transformed terrestrial organic matter on the outer shelf are slow ($< 3 \times 10^{-4}$ y^{-1}) and the overall terrestrial carbon burial efficiency is relatively high (> 87 %) and only slightly lower than previously reported based on millennial-scale carbon burial rates (> 90 %, Stein and Macdonald, 2004). Area-integrated rates of carbon mineralization in the outer shelf sediments (0.29 to 0.48 Tg y^{-1}) represent about 0.5 %

to 8 % of the annual terrestrial organic matter load to the Laptev and East Siberian Sea ranging from 6 Tg y^{-1} (Stein and Macdonald, 2004) to 22±8 to 44 Tg y^{-1} (Vonk et al., 2012). There are large uncertainties associated with these estimates, given that our calculations do not account for carbon mineralization of resuspended terrestrial organic material and likely higher rates of mineralization in the inner shelf sediments. Nevertheless, these data indicate that the contribution of the benthic DIC flux to the total CO_2 production in the outer Eastern Siberian Sea and Laptev Sea is small. This conclusion, however, does not necessarily extend to the inner parts of the Laptev Sea and the western parts of the East Siberian Sea, where CO_2 supersaturation has been reported by Semiletov et al. (2012) and Pipko et al. (2011). Anderson et al (2009) estimated a DIC excess of 10 Tg C by evaluating data from the Laptev and East Siberian Seas collected in the summer of 2008 and suggested that this excess was caused mainly by terrestrial organic matter decomposition. Their estimate can be compared to our sediment oxygen uptake for the outer Laptev and East Siberian Sea shelf of almost 16 Tg y^{-1}, which would demand that 62.5 % of the oxygen uptake was due to terrestrial organic matter mineralization. However, the reported annual production of marine organic matter for the total Laptev and East Siberian Sea is about 46 Tg y^{-1} (Stein and Macdonald, 2004). Even if only half of this amount is produced in the outer shelf region and only another half of that amount was deposited, there would still be more than 10 Tg y^{-1} of reactive marine organic matter at the sediment surface. Our data would therefore suggest that at least in the more productive East Siberian Sea the pronounced aragonite undersaturation reported for bottom waters in the East Siberian Sea is due to aerobic mineralization of a significant amount of marine organic matter, which extends the assessment for the western Chukchi Sea and the central Arctic Ocean by Qi et al. (2017). It is apparent that these sediments play a major role in the recycling of marine organic carbon on the Arctic shelf. Future changes in marine production on the Siberian shelf under longer ice-free conditions (Arrigo and van Dijken, 2011) will likely change the relative proportions of degrading marine and terrestrial organic matter further so that this particular shelf system may in the future more strongly resemble that of other ice-free shelf-slope environments.

6. Acknowledgements

Funding for this investigation came from the K&A Wallenberg foundation, the Swedish Polarsekretariat, and the Bolin Centre for Climate Research at Stockholm University. Igor

1296 Semiletov acknowledge support from the Russian Government (No.
1297 14.Z50.31.0012/03.19.2014). We would like to thank the members of the SWERUS-C3
1298 consortium, the shipcrew on icebreaker Oden, and Heike Siegmund, Lina Hansson, Barkas
1299 Charalampos, and Dimitra Panagiotopoulou for help with the laboratory work. We dedicate
1300 this publication to our friend and colleague Vladimir Samarkin, who unfortunately passed
1301 away before publication of this work. This manuscript benefitted from discussions with
1302 Patrick Crill, Örjan Gustafsson, Christoph Humborg, Julia Steinbach, Clint Miller, Marc
1303 Geibel, Emma Karlsson, Brett Thornton, Jorien Vonk, Leif Anderson, and Magnus Mörth.

1304

List of Tables

List of figures

1343 mixing model versus $\delta^{13}C_{DIC}$. The slope and y-intercept of the regression for each station are
1344 shown in Table 3.

1345

1346 Fig. 7 A, B. Map of field area and sampling stations showing oxygen uptake rates in panel A
1347 and depth-integrated sulfate reduction rates in panel B.

1348

1349 Fig. 8A. Water depth variation of sediment oxygen uptake. 8B: Water depth variation of
1350 integrated ^{35}S-sulfate reduction rates (0-30 cm sediment depth). For reference average rates of
1351 abyssal plain, continental rise, slope, and shelf sediments, deposition and non-depositional,
1352 are shown for reference.

1353

1354 Fig. 9. Crossplot of diffusive oxygen uptake and integrated sulfate reduction rates. The black
1355 line is the linear regression and yielded a y-intercept of 2.1 mmol m^{-2} d^{-1} and a slope of 5.55.
1356 Blue and red lines show the 95% and 99% confidence interval.

1357

1358

7. References

Alling, V., Sanchez-Garcia, L., Porcelli, D., Pugach, S., Vonk, J. E., van Dongen, B., Mörth, C.-M., Anderson, L. G., Sokolov, A., Andersson, P., Humborg, C., Semiletov, I., and Gustafsson, Ö.: Non-conservative behavior of dissolved organic carbon across the Laptev and East Siberian seas, Global Biogeochemical Cycles, 24, 10.1029/2010gb003834, 2010.

Alling, V., Porcelli, D., Mörth, C. M., Anderson, L. G., Sanchez-Garcia, L., Gustafsson, Ö., Andersson, P. S., and Humborg, C.: Degradation of terrestrial organic carbon, primary production and out-gassing of CO_2 in the Laptev and East Siberian Seas as inferred from $\delta^{13}C$ values of DIC, Geochimica et Cosmochimica Acta, 95, 143-159, 2012.

Anderson LG, Jutterström S, Hjalmarsson S, Wahlstrom I, Semiletov IP. Out-gassing of CO_2 from Siberian Shelf seas by terrestrial organic matter decomposition. Geophysical Research Letters, **36**, L20601, 2009.

Arrigo, K. R., and van Dijken, G. L.: Secular trends in Arctic Ocean net primary production, Journal of Geophysical Research: Oceans, 116, 10.1029/2011JC007151, 2011.

Bauch, D., Dmitrenko, I., Kirillov, S., Wegner, C., Hölemann, J., Pivovarov, S., Timokhov, L., and Kassens, H.: Eurasian Arctic shelf hydrography: Exchange and residence time of southern Laptev Sea waters, Continental Shelf Research, 29, 1815-1820, 2009.

Berg, P., Petersen-Risgaard, N., and Rysgaard, S.: Interpretation and measured concentration profiles in sediment pore water, Limnology and Oceanography, 43, 1500-1510, 1998.

Berg, P., Rysgaard, S., and Thamdrup, B.: Dynamic modeling of early diagenesis and nutrient cycling. A case study in an Arctic marine sediment, Amer. J. Sci, 303, 906-955, 2003.

Boetius, A., and Damm, E.: Benthic oxygen uptake, hydrolytic potentials and microbial biomass at the Arctic continental slope, Deep Sea Research Part I: Oceanographic Research Papers, 45, 239-275, 1998.

Boudreau, B. P.: Diagenetic models and their implementation, Springer Verlag, 414 pp., 1996.

1386 Bourgeois, S., Archambault, P., and Witte, U.: Organic matter remineralization in marine
1387 sediments: A Pan-Arctic synthesis, Global Biogeochemical Cycles, 31, 190-213, 2017.

1388 Bröder, L.-M., Tesi, T., Salvado, J. A., Semiletov, I., Dudarev, O. V., and Gustafsson, Ö.:
1389 Fate of terrigeneous organic matter across the Laptev Sea from the mouth of the Lena River to
1390 the deep sea of the Arctic interior, Biogeosciences, 13, 5003-5019, 2016a.

1391 Bröder, L., Tesi, T., Andersson, A., Eglinton, T. I., Semiletov, I. P., Dudarev, O. V., Roos, P.,
1392 and Gustafsson, Ö.: Historical records of organic matter supply and degradation status in the
1393 East Siberian Sea, Organic Geochemistry, 91, 16-30, 2016b.

1394 Canfield, D. E., Kristensen, E., and Thamdrup, B.: Aquatic geomicrobiology, Advances in
1395 marine biology, 48, 2005.

1396 Dmitrenko, I. A., Tyshko, K. N., Kirillov, S. A., Eicken, H., Hölemann, J. A., and Kassens,
1397 H.: Impact of flaw polynyas on the hydrography of the Laptev Sea, Global and Planetary
1398 Change, 48, 9-27, 2005.

1399 Dmitrenko, I. A., Kirillov, S. A., and Tremblay, L. B.: The long-term and interannual
1400 variability of summer fresh water storage over the eastern Siberian shelf: Implication for
1401 climatic change, Journal of Geophysical Research: Oceans, 113, doi: 10.1029/2007JC004304,
1402 2008.

1403 Dudarev, O. V., Semiletov, I. P., and Charkin, A. N.: Particulate material composition in the
1404 Lena River-Laptev Sea system: Scales of heterogeneities. In: Doklady Earth Sciences, 6,
1405 1000-1005, 2006.

1406 Fahl, K., and Nöthig, E.-M.: Lithogenic and biogenic particle fluxes on the Lomonosov Ridge
1407 (central Arctic Ocean) and their relevance for sediment accumulation: Vertical vs. lateral
1408 transport, Deep Sea Research Part I: Oceanographic Research Papers, 54, 1256-1272, 2007.

1409 Glud, R. N.: Oxygen dynamics of marine sediments, Mar. Biol. Res., 4, 243-289, 2008.

1410 Grebmeier, J. M., Cooper, L. W., Feder, H. M., and Sirenko, B. I.: Ecosystem dynamics of the
1411 Pacific-influenced Northern Bering and Chukchi Seas in the Amerasian Arctic, Progress in
1412 Oceanography, 71, 331-361, 2006.

Guay, C. K., Falkner, K. K., Muench, R. D., Mensch, M., Frank, M., and Bayer, R.: Wind-driven transport pathways for Eurasian Arctic river discharge, Journal of Geophysical Research: Oceans, 106, 11469-11480, 2001.

Guo, L., Ping, C. L., and Macdonald, R. W.: Mobilization pathways of organic carbon from permafrost to arctic rivers in a changing climate, Geophysical Research Letters, 34, 2007.

Hall, P. O. J., and Aller, R. C.: Rapid, small-volume flow injection analysis for ΣCO_2 and NH_4^+ in marine and freshwaters, Limnology and Oceanography, 37, 1113-1119, 1992.

Hugelius, G., Strauss, J., Zubrzycki, S., Harden, J. W., Schuur, E. A. G., Ping, C. L., Schirrmeister, L., Grosse, G., Michaelson, G. J., Koven, C. D., O'Donnell, J. A., Elberling, B., Mishra, U., Camill, P., Yu, Z., Palmtag, J., and Kuhry, P.: Estimated stocks of circumpolar permafrost carbon with quantified uncertainty ranges and identified data gaps, Biogeosciences, 11, 6573-6593, 2014.

Ivanov, V. V. and Golovin, P. N.: Observations and modeling of dense water cascading from the northwestern Laptev Sea shelf, Journal of Geophysical Research: Oceans, 112, 2007.

Jørgensen, B. B.: A comparison of methods for the quantification of bacterial sulfate reduction in coastal marine sediments: I. Measurement with radiotracer techniques, Geomicrobiology Journal, 1, 11-27, 1978.

Jørgensen, B. B., and Kasten, S.: Sulfur and methane oxidation, in: Marine Geochemistry, Second Edition ed., edited by: Schulz, H. D., and Zabel, M., Springer Verlag, Berlin Heidelberg, 271-309, 2006.

Kallmeyer, J., Ferdelman, T. G., Weber, A., Fossing, H., and Jørgensen, B. B.: Evaluation of a cold chromium distillation procedure for recovering very small amounts of radiolabeled sulfide related to sulfate reduction measurements., Limnol. Oceanog. Methods, 2, 171-180, 2004.

Karlsson, E. S., Brüchert, V., Tesi, T., Charkin, A., Dudarev, O., Semiletov, I., and Gustafsson, Ö.: Contrasting regimes for organic matter degradation in the East Siberian Sea and the Laptev Sea assessed through microbial incubations and molecular markers, Marine Chemistry, 170, 11-22, 2015.

1441 Koven, C. D., Lawrence, D. M., and Riley, W. J.: Permafrost carbon-climate feedback is
1442 sensitive to deep soil carbon decomposability but not deep soil nitrogen dynamics,
1443 Proceedings of the National Academies of Science, 112, 3752-3757, 2015.

1444 Lalonde, K., Mucci, A., Ouellet, A., and Gelinas, Y.: Preservation of organic matter in
1445 sediments promoted by iron, Nature, 483, 198-200, 2012.

1446 Li, Y.-H. and Gregory, S.: Diffusion of ions in sea water and in deep-sea sediments,
1447 Geochimica et Cosmochimica Acta, 88, 703-714, 1974.

1448 Macdonald, R. W., and Gobeil, C.: Manganese Sources and Sinks in the Arctic Ocean with
1449 Reference to Periodic Enrichments in Basin Sediments, Aquatic Geochemistry, 18, 565-591,
1450 2012.

1451 Mackin, J. E., and Aller, R.C.: Ammonium adsorption in marine sediments, Limnology and
1452 Oceanography, 29, 250-257, 1984.

1453 Macdonald, R. W., Kuzyk, Z. Z. A., and Johannessen, S. C.: The vulnerability of Arctic shelf
1454 sediments to climate change, Environmental Reviews, 1-19, 2015.

1455 McGuire, A. D., Anderson, L. G., Christensen, T. R., Dallimore, S., Guo, L., Hayes, D. J.,
1456 Heimann, M., Lorenson, T. D., Macdonald, R. W., and Roulet, N.: Sensitivity of the carbon
1457 cycle in the Arctic to climate change, Ecological Monographs, 79, 523-555, 2009.

1458 McTigue, N., Gardner, W., Dunton, K., and Hardison, A.: Biotic and abiotic controls on co-
1459 occurring nitrogen cycling processes in shallow Arctic shelf sediments, Nature
1460 Communications, 7, 2016.

1461 Miller, C. M., Dickens, G. R., Jakobsson, M., Johansson, C., Koshurnikov, A., O'Regan, M.,
1462 Muschitiello, F., Stranne, C., and Mörth, C.-M.: Low methane concentrations in sediment
1463 along the continental slope north of Siberia: Inference from pore water geochemistry,
1464 Biogeosciences Discussions, doi:10.5194/bg-2016-308, 2016.

1465 Naidu, A. S., Cooper, L. W., Finney, B. P., Macdonald, R. W., Alexander, C., and Semiletov,
1466 I. P.: Organic carbon isotope ratios ($\delta^{13}C$) of Arctic Amerasian Continental shelf sediments.
1467 International Journal of Earth Sciences, 89, 522-532, 2000.

1468 Nickel, M., Vandieken, V., Brüchert, V., and Jørgensen, B. B.: Microbial Mn(IV) and Fe(III)
1469 reduction in northern Barents Sea sediments under different conditions of ice cover and

organic carbon deposition, Deep Sea Research Part II: Topical Studies in Oceanography, 55, 2390-2398, 2008.

Nitishinsky, M., Anderson, L. G., and Hölemann, J. A.: Inorganic carbon and nutrient fluxes on the Arctic Shelf, Continental Shelf Research, 27, 1584-1599, 2007.

Pipko, I., Semiletov I.P., Pugach S.P., Wahlstrom I., Anderson L.G. Interannual variability of air-sea CO_2 fluxes and carbon system in the East Siberian Sea. Biogeosciences, **8**, 1987-2007, 2011.

Pivovarov, S., Hölemann, J., Kassens, H., Antonow, M., and Dmitrenko, I.: Dissolved oxygen,silicon,phosphorous and suspended matter concentrations during the spring breakup of the Lena River, in: Land–Ocean Systems in the Siberian Arctic:Dynamics and History, edited by: Kassens, H., Bauch, H. A., Dmitrenko, I., Eicken, H., Hubberten, H.-W., Melles, M., Thiede, J., and Timokhov, L., Springer, Berlin, 251-264, 1999.

Qi, D., Chen, L., Chen, B., Gao, Z., Zhong, W., Feely, R. A., Anderson, L. G., Sun, H., Chen, J., Chen, M., Zhan, L., Zhang, Y., and Cai, W.-J.: Increase in acidifying water in the western Arctic Ocean, Nature Clim. Change, 7, 195-199, 2017.

Rachold, V., Eicken, H., Gordeev, V., Grigoriev, M. N., Hubberten, H.-W., Lisitzin, A. P., Shevchenko, V., and Schirrmeister, L.: Modern terrigenous organic carbon input to the Arctic Ocean, in: The organic carbon cycle in the Arctic Ocean, Springer, 33-55, 2004.

Rasmussen, H., and Jørgensen, B. B.: Microelectrode studies of seasonal oxygen uptake in a coastal sediment: Role of molecular diffusion, Marine ecology progress series. Oldendorf, 81, 289-303, 1992.

Raymond, P. A., McClelland, J., Holmes, R., Zhulidov, A., Mull, K., Peterson, B., Striegl, R., Aiken, G., and Gurtovaya, T.: Flux and age of dissolved organic carbon exported to the Arctic Ocean: A carbon isotopic study of the five largest arctic rivers, Global Biogeochemical Cycles, 21, 10.1029/2007GB002983, 2007.

Rekant, P., Bauch, H. A., Schwenk, T., Portnov, A., Gusev, E., Spiess, V., Cherkashov, G., and Kassens, H.: Evolution of subsea permafrost landscapes in Arctic Siberia since the Late Pleistocene: a synoptic insight from acoustic data of the Laptev Sea, Arktos, 1, 10.1007/s41063-015-0011-y, 2015.

1499 Rossel, P. E., Bienhold, C., Boetius, A., and Dittmar, T.: Dissolved organic matter in pore
1500 water of Arctic Ocean sediments: Environmental influence on molecular composition,
1501 Organic Geochemistry, 97, 41-52, 2016.

1502 Sakshaug, E.: Primary and secondary production in the Arctic Seas, in: The organic carbon
1503 cycle in the Arctic Ocean, Springer, 57-81, 2004.

1504 Salvadó, J. A., Tesi, T., Andersson, A., Ingri, J., Dudarev, O. V., Semiletov, I. P., and
1505 Gustafsson, Ö.: Organic carbon remobilized from thawing permafrost is resequestered by
1506 reactive iron on the Eurasian Arctic Shelf, Geophysical Research Letters, 42, 8122-8130,
1507 2015.

1508 Sánchez-García, L., Alling, V., Pugach, S., Vonk, J., van Dongen, B., Humborg, C., Dudarev,
1509 O., Semiletov, I., and Gustafsson, Ö.: Inventories and behavior of particulate organic carbon
1510 in the Laptev and East Siberian seas, Global Biogeochemical Cycles, 25,
1511 10.1029/2010gb003862, 2011.

1512 Savvichev, A., Rusanov, I., Pimenov, N., Zakharova, E., Veslopolova, E., Lein, A. Y., Crane,
1513 K., and Ivanov, M.: Microbial processes of the carbon and sulfur cycles in the Chukchi Sea,
1514 Microbiology, 76, 603-613, 2007.

1515 Schuur, E. A. G., McGuire, A. D., Schadel, C., Grosse, G., Harden, J. W., Hayes, D. J.,
1516 Hugelius, G., Koven, C. D., Kuhry, P., Lawrence, D. M., Natali, S. M., Olefeldt, D.,
1517 Romanovsky, V. E., Schaefer, K., Turetsky, M. R., Treat, C. C., and Vonk, J. E.: Climate
1518 change and the permafrost carbon feedback, Nature, 520, 171-179, 2015.

1519 Seeberg-Elverfeldt, J., Schlüter, M., Feseker, T., and Kölling, M.: Rhizon sampling of
1520 porewaters near the sediment-water interface of aquatic systems, Limnol. Oceanogr. Methods,
1521 3, 361-371, 2005.

1522 Semiletov, I., Dudarev, O., Luchin, V., Charkin, A., Shin, K.-H., and Tanaka, N.: The East
1523 Siberian Sea as a transition zone between Pacific-derived waters and Arctic shelf waters,
1524 Geophysical Research Letters, 10.1029/2005GL022490, 2005.

1525 Semiletov, I., Pipko, I., Gustafsson, Ö., Anderson, L. G., Sergienko, V., Pugach, S., Dudarev,
1526 O., Charkin, A., Gukov, A., Broder, L., Andersson, A., Spivak, E., and Shakhova, N.:
1527 Acidification of East Siberian Arctic Shelf waters through addition of freshwater and
1528 terrestrial carbon, Nature Geoscience, 9, 361-365, 2016.

Semiletov I.P., Shakhova, N.E, Pipko, I.I.: Space-time dynamics of carbon and environmental parameters related to carbon dioxide emissions in the Buor-Khaya Bay and adjacent part of the Laptev Sea. Biogeosciences, **10**, 5977-5996, 2013.

Semiletov I.P., Pipko I.I., Shakhova N.E., Dudarev O.V., Pugach S.P., Charkin A.N., McRoy C.P., Kosmach D., and Ö. Gustafsson.: Carbon transport by the Lena River from its headwaters to the Arctic Ocean, with emphasis on fluvial input of terrestrial particulate organic carbon vs. carbon transport by coastal erosion. Biogeosciences, **8**, 2407-2426, 2011.

Semiletov, I.P., Destruction of the coastal permafrost ground as an important factor in biogeochemistry of the Arctic Shelf waters, Trans. (Doklady) Russian Acad. Sci., 368, 679-682, 1999 (translated into English).

Stein, R., and Macdonald, R. W.: The Organic Carbon Cycle in the Arctic Ocean, Springer-Verlag, Berlin, 382 pp., 2004.

Strobl, C., Schulz, V., Vogler, S., Baumann, S., Kassens, H., Kubik, P. W., Suter, M., and Mangini, A.: Determination of depositional beryllium-10 fluxes in the area of the Laptev Sea and beryllium-10 concentrations in water samples of high northern latitudes, in: Land-Ocean Systems in the Siberian Arctic: Dynamics and History, edited by: Kassens, H., Bauch, H. A., Dmitrenko, I., Eicken, H., Hubberten, H.-W., Melles, M., Thiede, J., and Timokhov, L., Springer, Berlin, 515-532, 1998.

Tarnocai, C., Canadell, J. G., Schuur, E. A. G., Kuhry, P., Mazhitova, G., and Zimov, S.: Soil organic carbon pools in the northern circumpolar permafrost region, Global Biogeochemical Cycles, 23, 10.1029/2008gb003327, 2009.

Tesi, T., Semiletov, I., Hugelius, G., Dudarev, O., Kuhry, P., and Gustafsson, Ö.: Composition and fate of terrigenous organic matter along the Arctic land–ocean continuum in East Siberia: Insights from biomarkers and carbon isotopes, Geochimica et Cosmochimica Acta, 133, 235-256, 2014.

Tesi, T., Semiletov, I., Dudarev, O., Andersson, A., and Gustafsson, Ö.: Matrix association effects on hydrodynamic sorting and degradation of terrestrial organic matter during cross-shelf transport in the Laptev and East Siberian shelf seas, Journal of Geophysical Research: Biogeosciences, 121, 731-752, 2016.

1558 Thamdrup, B.: Bacterial manganese and iron reduction in aquatic sediments, Advances in
1559 Microbial Ecology, 16, 41-84, 2000.

1560 Arrigo, K. R., and van Dijken, G. L.: Secular trends in Arctic Ocean net primary production,
1561 Journal of Geophysical Research: Oceans, 116, 10.1029/2011JC007151, 2011.

1562 Hugelius, G., Strauss, J., Zubrzycki, S., Harden, J. W., Schuur, E. A. G., Ping, C. L.,
1563 Schirrmeister, L., Grosse, G., Michaelson, G. J., Koven, C. D., O'Donnell, J. A., Elberling, B.,
1564 Mishra, U., Camill, P., Yu, Z., Palmtag, J., and Kuhry, P.: Estimated stocks of circumpolar
1565 permafrost carbon with quantified uncertainty ranges and identified data gaps,
1566 Biogeosciences, 11, 6573-6593, 2014.

1567 Qi, D., Chen, L., Chen, B., Gao, Z., Zhong, W., Feely, R. A., Anderson, L. G., Sun, H., Chen,
1568 J., Chen, M., Zhan, L., Zhang, Y., and Cai, W.-J.: Increase in acidifying water in the western
1569 Arctic Ocean, Nature Clim. Change, 7, 195-199, 2017.

1570 Sánchez-García, L., Alling, V., Pugach, S., Vonk, J., van Dongen, B., Humborg, C., Dudarev,
1571 O., Semiletov, I., and Gustafsson, Ö.: Inventories and behavior of particulate organic carbon
1572 in the Laptev and East Siberian seas, Global Biogeochemical Cycles, 25,
1573 10.1029/2010gb003862, 2011.

1574 Vandieken, V., Nickel, M., and Jørgensen, B. B.: Carbon mineralization in Arctic sediments
1575 northeast of Svalbard: (Mn(IV) and Fe(III) reduction as principal anaerobic respiratory
1576 pathways, Marine Ecology Progress Series, 322, 15-27, 2006.

1577 Vonk, J. E., Sanchez-Garcia, L., van Dongen, B. E., Alling, V., Kosmach, D., Charkin, A.,
1578 Semiletov, I. P., Dudarev, O. V., Shakhova, N., Roos, P., Eglinton, T. I., Andersson, A., and
1579 Gustafsson, O.: Activation of old carbon by erosion of coastal and subsea permafrost in Arctic
1580 Siberia, Nature, 489, 137-140.

1581 Wegner, C., Hölemann, J. A., Dmitrenko, I., Kirillov, S., and Kassens, H.: Seasonal variations
1582 in Arctic sediment dynamics—evidence from 1-year records in the Laptev Sea (Siberian
1583 Arctic), Global and Planetary Change, 48, 126-140, 2005.

1584 Wegner, C., Bauch, D., Hölemann, J. A., Janout, M. A., Heim, B., Novikhin, A., Kassens, H.,
1585 and Timokhov, L.: Interannual variability of surface and bottom sediment transport on the
1586 Laptev Sea shelf during summer, Biogeosciences, 10, 1117-1129, 2013.

Weingartner, T. J., Danielson, S., Sasaki, Y., Pavlov, V., and Kulakov, M.: The Siberian Coastal Current: A wind- and buoyancy-forced Arctic coastal current, Journal of Geophysical Research: Oceans, 104, 29697-29713, 1999.

Table 1. Physical and chemical characteristics of sediment and bottom water at the sampled stations

Station	Latitude °N	Longitude °E	Date	Water depth	Ice cover	Bottom water salinity	Bottom water temperature	Bottom water O_2 concentration	Bottom water NH_4^+ concentration	Bottom water DIC above sediment	$\delta^{13}C$ DIC bottom water	Sediment description
			Month/Day/Year	m	%	‰	°C	µmol/L	µmol/L	µmol/L	‰ vs. VPDB	
1	78.942	125.243	7/15/2014	3146	50 - 75	34.9	-0.9	271.9	1.65	2151.5	-0.5	clay, brown
2	78.581	125.607	7/16/2014	2900	25 - 50	34.9	-0.9	275.0		n.a.	n.a.	clay, brown
3	78.238	126.150	7/16/2014	2601	< 25	34.9	-0.9	280.0		n.a.	n.a.	clay, brown
4	77.855	126.664	7/16/2014	2106	< 25	34.9	-0.8	289.4	1.81	2164.5	-1.6	clay, brown
6	77.142	127.378	7/17/2014	89	0.0	34.6	-1.8	327.0	1.30	2213.0	-2.2	clay, top 3 cm brown, then gray, fauna on top of sediment
23	76.171	129.333	7/22/2014	56	0.0	34.2	-1.8	303.2	1.34	2246.3	-3.2	silty clay, top 4 cm brown, then gray, brittle stars
24	75.599	129.558	7/24/2014	46	0.0	34.0	-1.7	283.8	0.89	2244.1	-2.0	silty clay, top 4 cm brown, then gray
27	76.943	132.229	7/23/2014	44	0.0	34.2	-1.8	332.3	0.94	2595.0	-6.5	silty clay, top 2 cm brown, then gray, fluffy surface layer, brittle stars
30	78.181	138.354	7/24/2014	69	0.0	34.1	-1.6	334.8	0.79	2178.4	-3.7	silty clay, top 4 cm brown, then gray
31	79.396	135.497	7/25/2014	3056	0.0	34.9	-0.9	270.9	0.74	2161.7	n.a.	clay, brown
35	78.600	137.061	7/26/2014	541	0.0	34.9	0.4	288.1	0.43	2183.7	n.a.	clay top 15cm brown, fluffy, inhomogeneous, surface-dwelling fauna
37	78.521	137.170	7/26/2014	205	0.0	34.7	0.0	295.4	0.89	2171.1	n.a.	clay, top 5cm brown, then gray
40	77.670	144.668	7/27/2014	45	0.0	31.5	-1.3	190.3	0.53	2213.7	-1.6	silty clay, top 3cm brown, then gray, brittle stars
43	76.780	147.791	7/28/2014	42	25-50	30.1	-1.2	256.4	0.61	2086.7	n.a.	silty clay to clayey silt, top 2cm brown, then gray, some small durface-dwelling animals
45	76.416	148.115	7/29/2014	40	< 50	29.1	-1.3	319.9	0.57	2576.0	-2.1	silty clay to clayey silt, 2cm brown, then gray-black, rather stiff
48	76.615	153.345	7/30/2014	49	> 75	30.6	-1.6	315.9	0.50	2075.1	-2.2	silty clay to clayey silt, top 3cm brown, then grayblack
50	75.764	158.529	8/1/2014	44	> 75	31.1	-1.4	311.0	0.51	2068.7	-2.1	silty clay to clayet silt, top 2cm brown, then grayblack
53	74.957	161.088	8/2/2014	47	> 75	31.0	-1.6	253.3	0.16	2086.1	-2.5	silty clay to clayey silt, top 3 cm brown, then 3 cm gray, then grayblack
58	74.440	166.050	8/4/2014	54	> 75	31.4	-1.7	254.3	0.65	2154.9	-1.5	silty clay to clayey silt, slightly resuspended, top 2 cm brown, then gray, soft
63	74.685	172.361	8/7/2014	67	> 75	32.4	-1.4	186.0	0.61	2240.8	-2.2	silty clay to clayey silt, top 1cm brown, then gray

1595

Table 2. O_2 uptake, integrated ^{35}S-sulfate reduction rates, DIC flux, and porewater DIC/NH_4^+ ratios

Station	Water depth	mean O_2 penetration depth	mean O_2 at 60mm depth	O_2 uptake (modelled/measured with 2D optode)	^{35}S-SRR (0-30 cm) duplicates	DIC flux (modelled in anaerobic zone/measured with whole core incubation)	Average porewater DIC/NH_4^+
	m	mm	µmol/L	mmol m^{-2} d^{-1}	mmol m^{-2} d^{-1}	mmol m^{-2} d^{-1}	
1	3146	> 60	217	1.48 ± 0.08	0.05 / 0.21	-0.11	
2	2900	> 60	213	1.32 ± 0.05			
3	2601	> 60	194	0.81 ± 0.06			
4	2106	> 60	89	1.32 ± 0.05	0.17 / 0.17	-0.15	
6	89	36	0	2.61 ± 0.01	0.03 / 0.05	-0.08	
23	56	13	0	5.00 ± 0.09 ; 5.3 ± 0.2	0.56	-0.12; -5.1 ± 0.4	13
24	46	10	0	7.95 ± 0.14		-0.22	10
27	44	16	0	3.75 ± 0.08	0.37 / 0.20	-0.27	12
30	69	16	0	2.61 ± 0.11	0.06 / 0.03	-0.12	15
31	3056	> 60	194	1.78 ± 0.07			
35	541	> 60	30	2.43 ± 0.32			
37	205	44	0	2.51 ± 0.10			
Average Laptev Sea shelf				**4.20**	**0.19**	**0.2 ; 5.1**	**12**
40	45	12	0	4.62 ± 0.08	0.33 / 0.24	-0.19	16
43	42	13	0	4.7 ± 0.10			
45	40	10	0	4.02 ± 0.10	0.23 / 0.19	-0.37	13
48	49	5	0	9.14 ± 0.22	0.68 / 0.53	-0.71	10
50	44	9	0	5.65 ± 0.43; 5.2 ± 0.1	1.32 / 1.40	-1.01 ; -5.2 ± 0.2	12
53	47	10	0	4.53 ± 0.08 ; 4.7 ± 0.1	0.10 / 0.17	-0.20	14
58	54	3	0	11.49 ± 0.52	1.01	-1.27	24
63	67	4	0	0.72 ± 0.15 ; 10.8 ± 0.2	1.41	-1.35 ; -10.8 ± 0.6	12
Average East Siberian Sea shelf				**7.2**		**0.7 ; 8.0**	**14**

1596

1597

1598

1599

Table 3. Anaerobic rates of carbon mineralization by manganese, iron, and sulfate reduction

	Net Fe^{2+} production	Net Mn^{2+} production	C-equivalent Fe + Mn reduction	^{35}S-Sulfate reduction	C-equivalents total anaerobic mineralization	Oxygen uptake	% Fe + Mn reduction of total anaerobic	Percentage anaerobic C mineralization of total	Percentage Fe and Mn mineralization of total
	mmol m^{-1} d^{-1}						%		
Station 23	0.05	0.03	0.03	0.56	1.1	5.0	2.3	22.9	0.5
Station 30	0.02	0.04	0.03	0.05	0.1	2.6	21.9	4.4	1.0
Station 45	0.14	0.12	0.09	0.21	0.5	4.0	18.3	12.8	2.3
Station 53	0.15	0.09	0.08	0.14	0.4	4.5	23.7	7.8	1.8
Station 63	-	0.50	0.25	1.41	3.1	10.7	8.1	26.0	2.3

1600

1601

Table 4. Calculated carbon isotope composition of remineralized DIC and mass fractions of the marine and terrestrial endmembers and corresponding terrestrial carbon degradation rates based on ^{35}S-SRR and DIC flux

Station	Average $\delta^{13}C_{DIC}$ remineralized	Marine end member	Terrestrial end member	^{35}S-SRR-based terrestrial degradation rate	DIC-based terrestrial degradation rate
	‰ vs. VPDB	Mass fraction		mmol m^{-2} d^{-1}	mmol m^{-2} d^{-1}
1	-35.8	0.0	1.0	0.13	0.11
4	-24.7	0.73	0.27	0.05	0.04
6	-25.1	0.65	0.35	0.01	0.03
23	-24.5	0.78	0.22	0.12	0.03
24	-24.7	0.73	0.27		0.06
27	-25.4	0.58	0.42	0.12	0.11
30	-28.5	0.00	1.00	0.05	0.13
Average Laptev Sea shelf	**-25.6**	**0.53**	**0.47**	**0.08**	**0.07**
40	-21.4	0.72	0.28	0.08	0.05
45	-22.2	0.63	0.37	0.08	0.14
48	-23.0	0.54	0.46	0.28	0.32
50	-24.0	0.43	0.57	0.77	0.57
53	-18.8	1.00	0.00	0.00	0.00
58	-22.6	0.59	0.41	0.42	0.53
63	-20.3	0.84	0.16	0.25	0.22
Average East Siberian Sea shelf	**-21.8**	**0.68**	**0.32**	**0.27**	**0.26**

1602

Table 5. Regional estimates of sediment carbon mineralization in the outer Laptev and East Siberian shelf sea

			Dissolved O_2 uptake	Upward DIC flux (anaerobic)	Terrestrial OC-derived DIC flux (anaerobic)	Marine OC-derived DIC flux (anaerobic)	Depth-integrated ^{35}S-SRR (C equivalent)
Outer Laptev Sea	**Average**	**mmol m^{-2} d^{-1}**	4.2	0.16	0.07	0.09	0.09
Outer East Siberian Sea	**Average**	**mmol m^{-2} d^{-1}**	7.2	0.73	0.26	0.47	0.34
Outer Laptev Sea	**280,000 km^2**	**Tg C y^{-1}**	5.2	0.20	0.09	0.11	0.11
Outer East Siberian Sea	**340,000 km^2**	**Tg C y^{-1}**	10.8	1.09	0.39	0.70	0.50
Total outer shelf area	**620,000 km^2**	**Tg C y^{-1}**	15.9	1.28	0.48	0.81	0.62

			^{35}S-SRR-based terrestrial C degradation	^{35}S-SRR-based marine C degradation	Total TEAP-based anaerobic OC degradation rate	Total TEAP-based anaerobic terrestrial OC degradation rate	Total TEAP-based anaerobic marine OC degradation rate
Outer Laptev Sea	**Average**	**mmol m^{-2} d^{-1}**	0.04	0.05	0.15	0.05	0.10
Outer East Siberian Sea	**Average**	**mmol m^{-2} d^{-1}**	0.13	0.21	0.42	0.16	0.26
Outer Laptev Sea	**280,000 km^2**	**Tg C y^{-1}**	0.05	0.07	0.18	0.06	0.12
Outer East Siberian Sea	**340,000 km^2**	**Tg C y^{-1}**	0.20	0.31	0.62	0.23	0.39
Total outer shelf area	**620,000 km^2**	**Tg C y^{-1}**	0.25	0.37	0.80	0.29	0.51

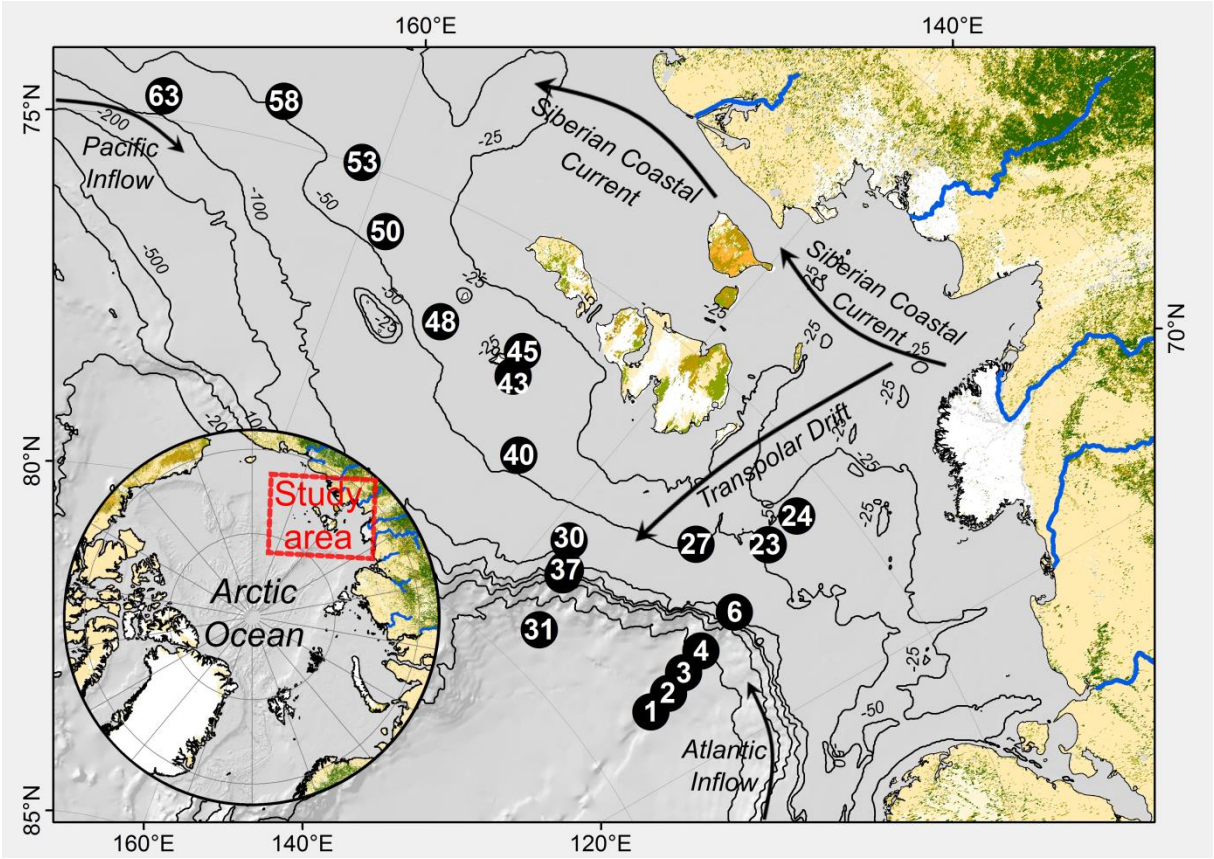

1604

1605 Fig. 1. Map of the Eastern Siberian Sea and slope and station locations.

1606

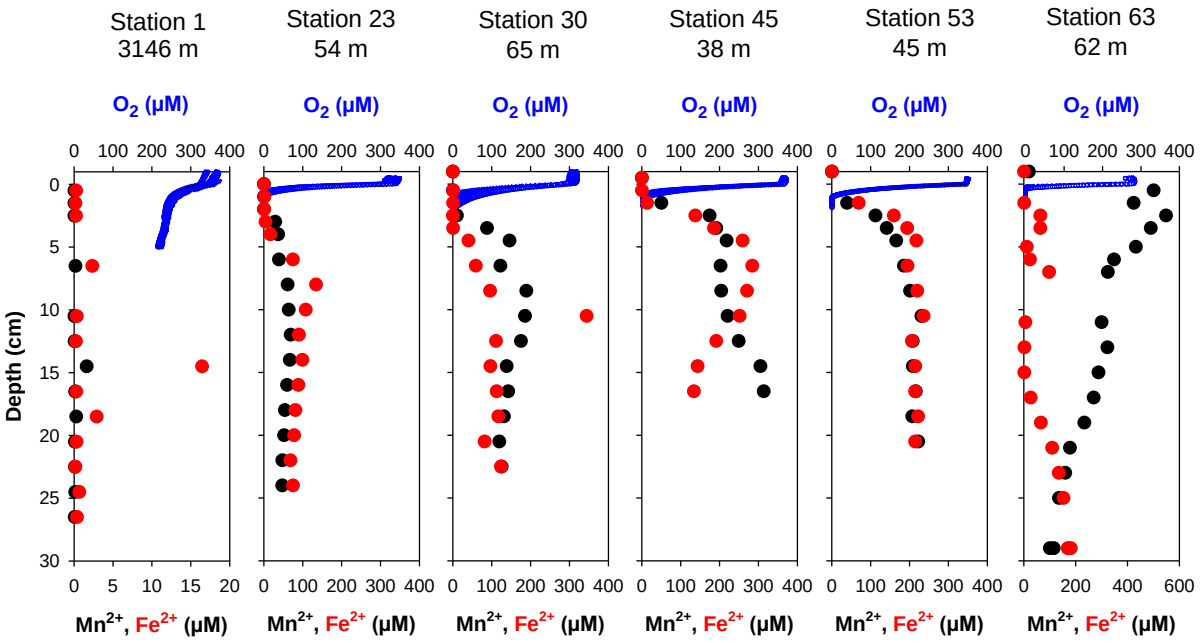

Fig. 2. Depth profiles of dissolved O_2, Fe^{2+}, and Mn^{2+} at Stations 1, 23, 30, 45, 53, and 63. For microelectrode profiles, 4 replicates are shown for each station. Depth resolution of measurement for O_2 was 100 µm.

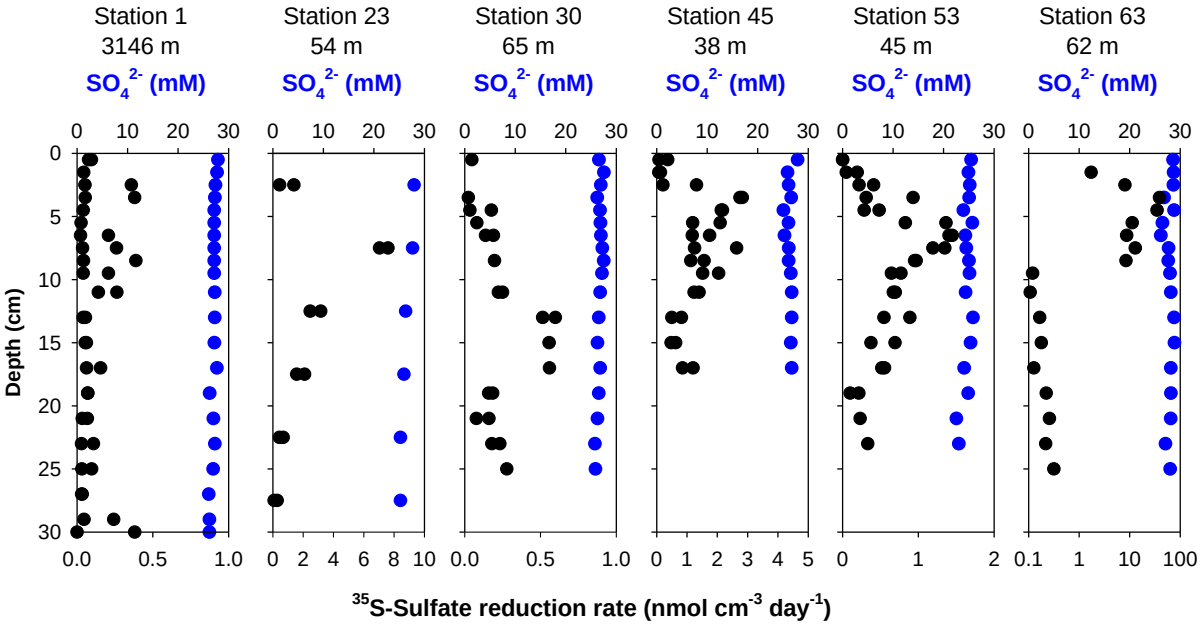

Fig. 3. Depth of profiles of ^{35}S-sulfate reduction rates and porewater concentration of dissolved sulfate for Stations 1, 23, 30, 45, 53, and 63. A replicate incubation was conducted for each depth except for Station 63.

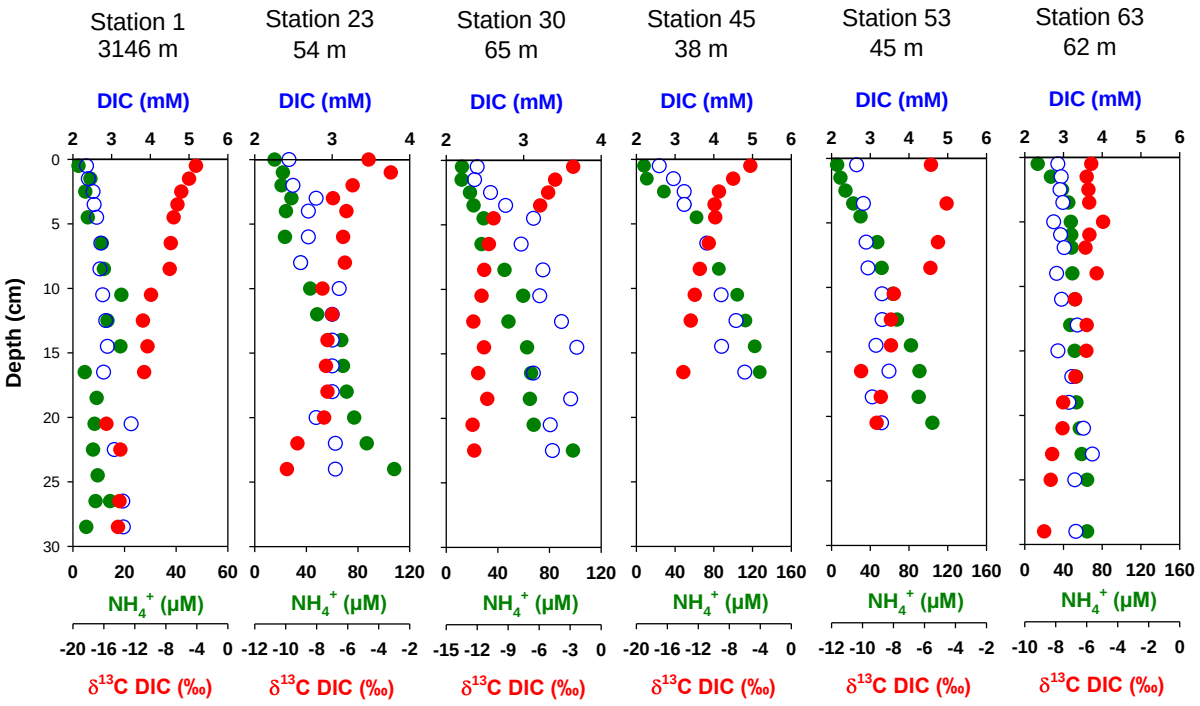

1618

1619 Fig. 4. Depth profiles of porewater dissovled inorganic carbon (DIC), δ^{13}C DIC and porewater NH_4^+ at
1620 stations 1, 23, 30, 45, 53, and 63.

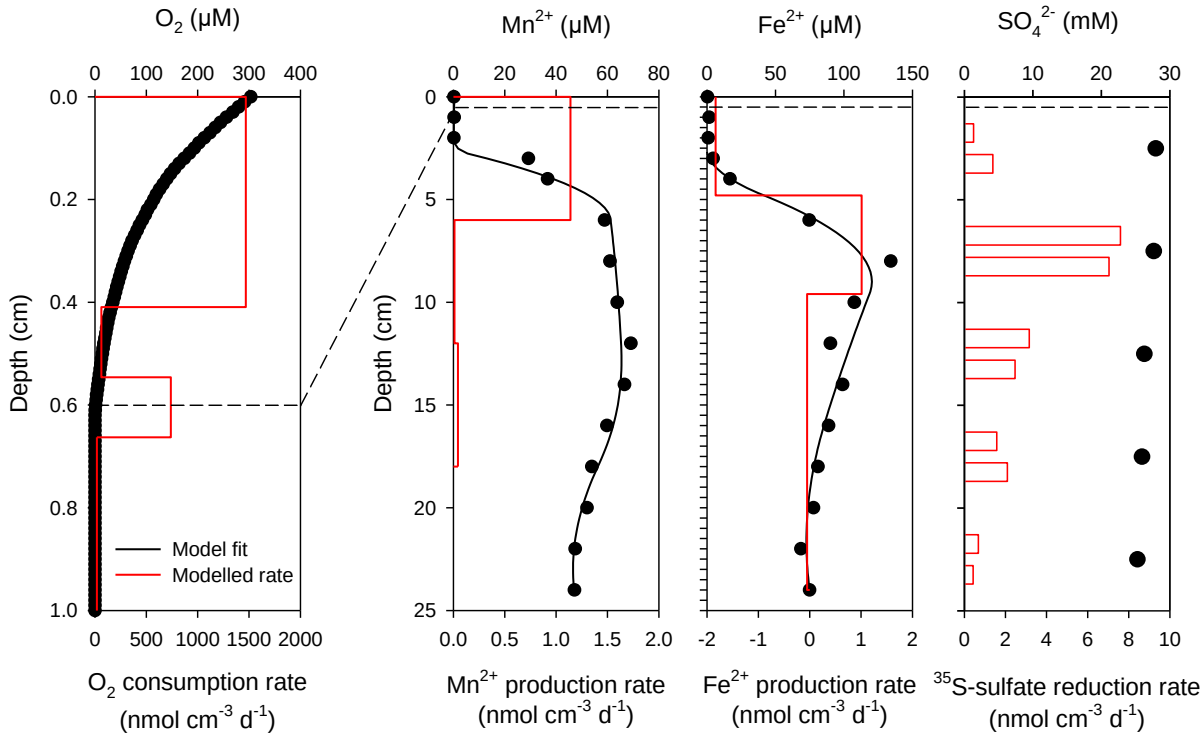

1621

1622 Fig. 5. Comparison of reaction rates of oxygen, manganese, iron, and sulfate reduction at Station 23.
1623 Note the different depth scale for the O_2 consumption rate. The dashed line marks the oxygen
1624 penetration depth.

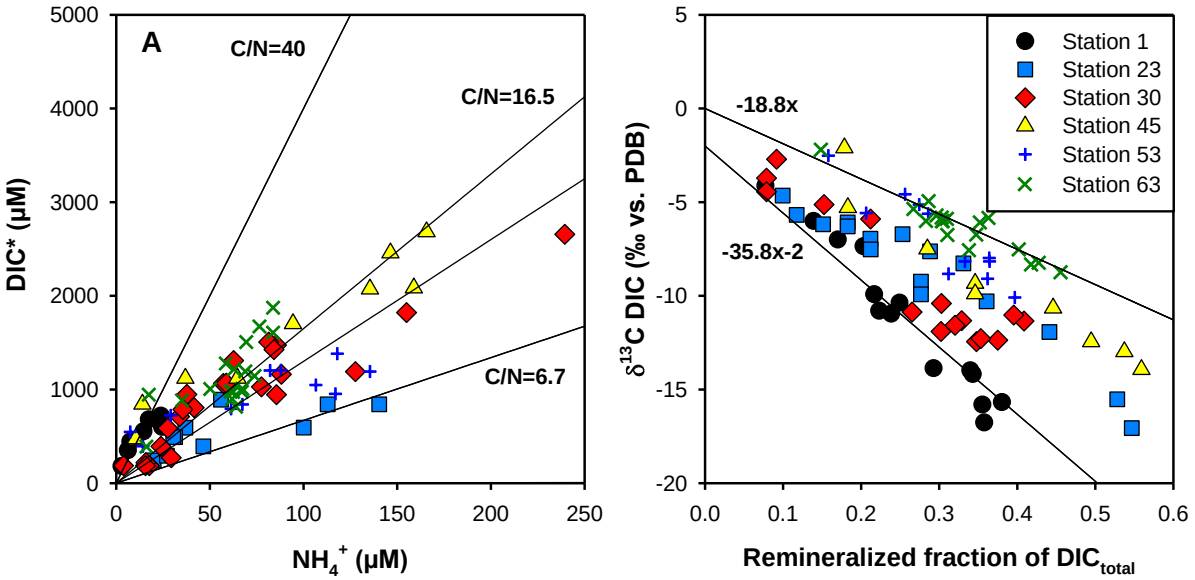

Fig. 6. A: Crossplot of dissolved NH_4^+ and porewater DIC* after correction for bottom water DIC concentrations. The slopes of the regression lines for the individual stations are shown in Table 2. B: Crossplot of the fraction of remineralized DIC calculated from a 2-endmember mixing model versus $\delta^{13}C$ DIC. The slope and y-intercept of the regression for each station are shown in Table 3.

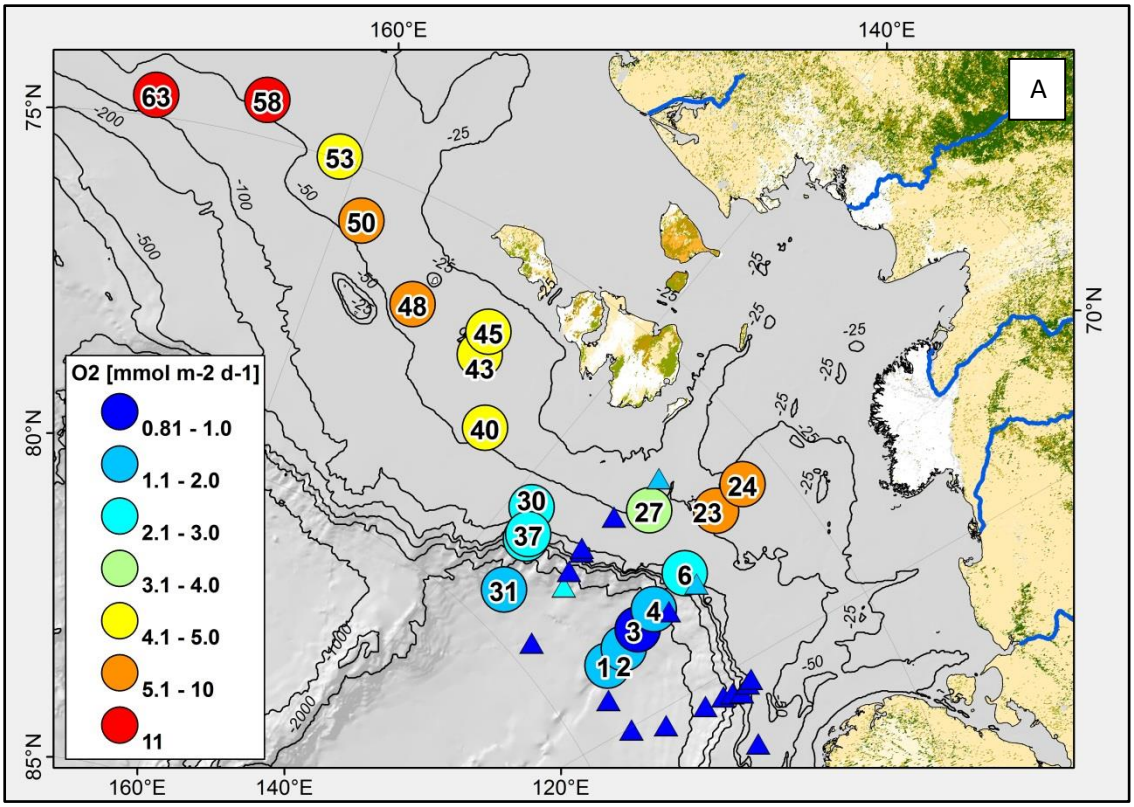

1633

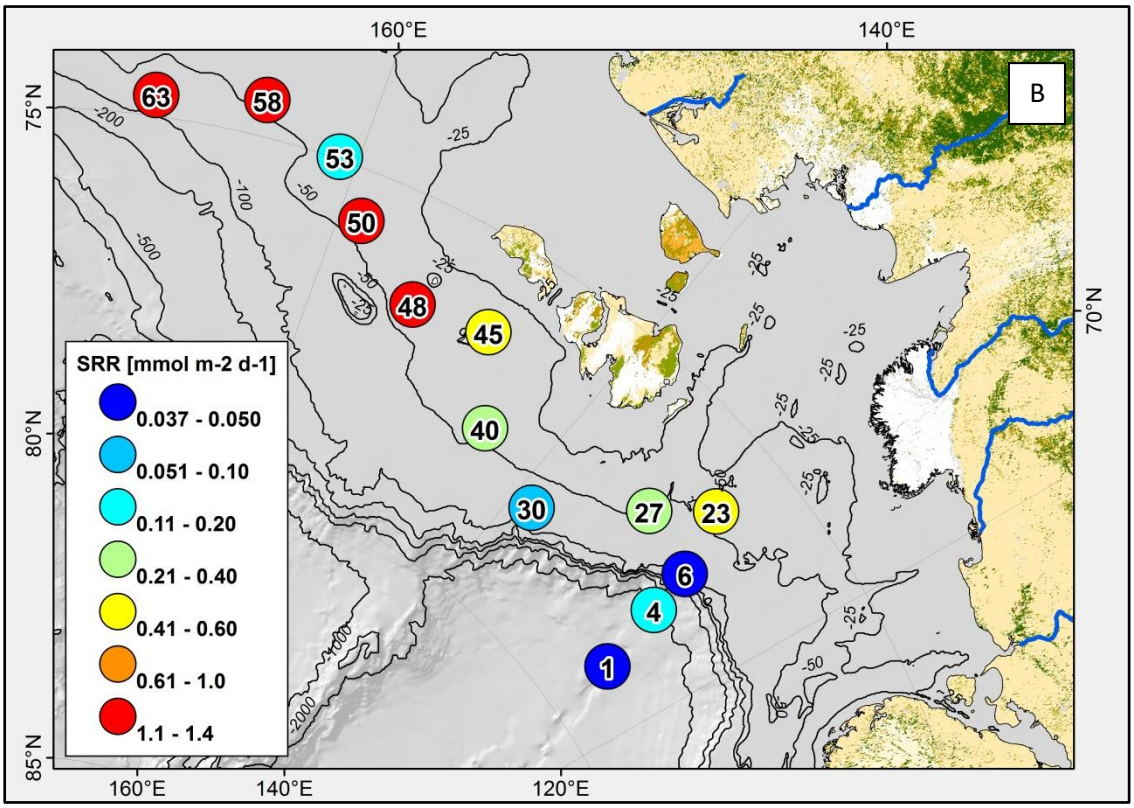

1634

1635 Fig. 7 A, B. Map of field area and sampling stations showing oxygen uptake rates in panel A and
1636 depth-integrated sulfate reduction rates in panel B.

1637

1638

1639

1640

1641

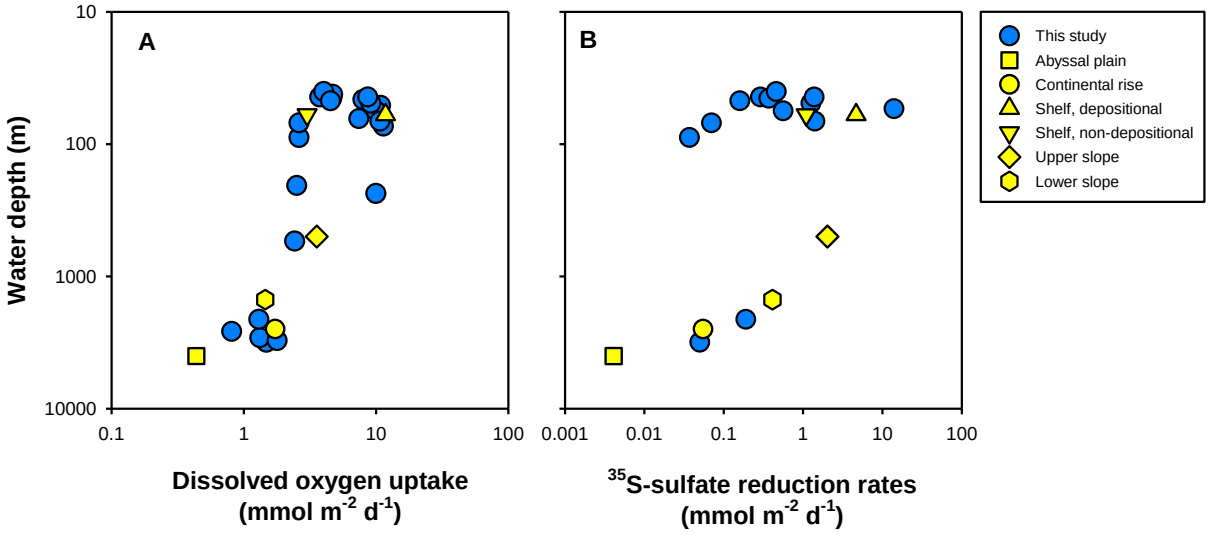

1642

1643 Fig. 8A. Water depth variation of sediment oxygen uptake. 8B: Water depth variation of integrated

1644 ^{35}S-sulfate reduction rates (0-30 cm sediment depth). For reference average rates of abyssal plain,

1645 continental rise, slope, and shelf sediments, deposition and non-depositional from Canfield et al.

1646 (2005).

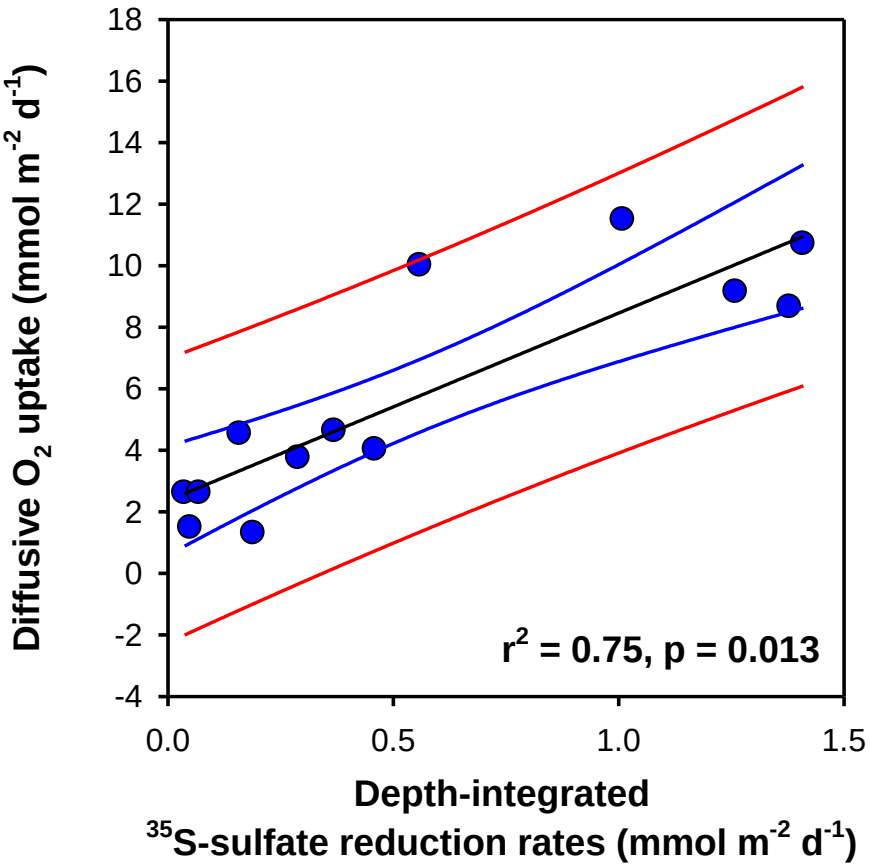

Fig. 9. Crossplot of diffusive oxygen uptake and integrated sulfate reduction rates. The black line is the linear regression and yielded a y-intercept of 2.1 mmol m^{-2} d^{-1} and a slope of 5.55. Blue and red lines show the 95% and 99% confidence interval.